NASA TECHNICAL NOTE

NASA TN D-7371

NASA TN D-7371

LEADING-EDGE SERRATIONS WHICH REDUCE THE NOISE OF LOW-SPEED ROTORS

by Paul T. Soderman

Ames Research Center and
U.S. Army Air Mobility R&D Laboratory
Moffett Field, Calif. 94035

NATIONAL AERONAUTICS AND SPACE ADMINISTRATION • WASHINGTON, D. C. • AUGUST 1973

1. Report No.	2. Government Accession No.	3. Recipient's Catalog No.
NASA TN D-7371		

4. Title and Subtitle	5. Report Date
LEADING-EDGE SERRATIONS WHICH REDUCE THE NOISE OF LOW-SPEED ROTORS	August 1973
	6. Performing Organization Code

7. Author(s)	8. Performing Organization Report No.
Paul T. Soderman	A-4074
	10. Work Unit No.
9. Performing Organization Name and Address	136-13-01-08-00-21
NASA Ames Research Center and U. S. Army Air Mobility R&D Laboratory Moffett Field, California 94035	11. Contract or Grant No.
	13. Type of Report and Period Covered
12. Sponsoring Agency Name and Address	Technical Note
National Aeronautics and Space Administration Washington, D. C. 20546	14. Sponsoring Agency Code

15. Supplementary Notes

16. Abstract

Acoustic effects of serrated brass strips attached near the leading edges of two different size rotors were investigated. The two-bladed rotors were tested in hover. Rotor rotational speed, blade angle, serration shape, and serration position were varied. The serrations were more effective as noise suppressors at rotor tip speeds less than 135 m/sec (444 ft/sec) than at higher speeds. High frequency noise was reduced but the low frequency rotational noise was little affected. Noise reductions from 4 to 8 dB overall sound pressure level and 3 to 17 dB in the upper octave bands were achieved on the 1.52 m (5.0 ft) diameter rotor. Noise reductions up to 4 dB overall sound pressure level were measured for the 2.59 m (8.5 ft) diameter rotor at some conditions.

17. Key Words (Suggested by Author(s))	18. Distribution Statement
Leading-edge serration Rotor noise Aerodynamic noise Owl wing Vortex generator	Unclassified – Unlimited

19. Security Classif. (of this report)	20. Security Classif. (of this page)	21. No. of Pages	22. Price*
Unclassified	Unclassified	65	$3.00

* For sale by the National Technical Information Service, Springfield, Virginia 22151

SYMBOLS

C_Q	torque coefficient, $\frac{Q}{\pi\rho R^3 V_T^2}$
C_T	thrust coefficient, $\frac{T}{\pi\rho R^2 V_T^2}$
Fm	figure of merit, $0.707\frac{C_T^{1.5}}{C_Q}$
N	rotational speed, rpm
Q	torque, J (ft-lb)
R	radius, m (ft)
T	thrust, N (lb force)
V_T	tip speed, m/sec (ft/sec)
β	blade angle measured at 0.75 radius station relative to a plane perpendicular to the rotor axis, deg
ρ	density, kg/m^3 (slug/ft^3)
σ	solidity, $\frac{\text{blade area}}{\text{disc area}}$ (0.105 for large rotor)

LEADING-EDGE SERRATIONS WHICH REDUCE THE NOISE OF LOW-SPEED ROTORS

Paul T. Soderman

Ames Research Center and
U. S. Army Air Mobility R&D Laboratory

SUMMARY

The acoustic effects of serrated brass strips attached to a small-scale and a large-scale rotor were measured. The rotors were tested in a simulated hover condition with the thrust axis parallel to the ground. Thrust and torque of the large-scale rotor were measured.

The small-scale rotor was 1.52 m (5.0 ft) in diameter; it had two blades with 6.99 cm (2.75 in.) chords and NACA 0012 airfoil sections. The large-scale rotor was 2.59 m (8.5 ft) in diameter; it had two blades with 21.34 cm (8.4 in.) chords and NACA 0015 airfoil sections. The serrations were attached to the underside of each blade near the leading edge. The small-scale rotor was tested at blade angles of 4°, 8°, 10°, and 12° and rotational speeds ranging from 480 to 1440 rpm, which correspond to tip Reynolds numbers of 183,000 to 550,000. The results of the small-scale rotor study are applicable to low-speed rotating blades or the inboard sections of high-tip-speed blades. The large-scale rotor had tip Reynolds numbers which approximated those of conventional rotors and propellers. That rotor was tested at blade angles of 6°, 12°, and 18° and rotational speeds ranging from 500 to 1600 rpm, which correspond to tip Reynolds numbers of 994,000 to 3,180,000.

The serrations were effective in reducing the high frequency noise of the rotors but not the low frequency rotational noise. Noise reductions from 4 to 8 dB overall sound pressure level and 3 to 17 dB in the high octave bands were achieved on the small-scale rotor. Noise reductions up to 4 dB overall sound pressure level were measured for the large-scale rotor at 800 and 1000 rpm.

Rotor performance was essentially unchanged by the presence or absence of serrations on the blades.

INTRODUCTION

Ornithologists have known for a long time that owls fly very quietly in pursuit of their prey. References 1 and 2 suggest that serrated feathers on the leading edge of the owl's wing are partly responsible for the low noise level of the owl. Figure 1 shows the wing and serrated feathers of a barn owl (tyto alba). Investigations were started on the effects of serrations on the noise generation and performance of rotating propulsive machinery.

This paper reports the results of acoustic tests of a small-scale and a large-scale rotor with leading-edge serrations modeled after the owl feather. The two-bladed rotors were tested in hover conditions (thrust axis parallel to the ground). Some of the data from the small-scale rotor test have been presented in reference 3. The work reported here has led to detailed studies by this author (ref. 4), by Hersh and Hayden (ref. 5), and by Arndt and Nagel (ref. 6) into the aeracoustic mechanisms involved with serrated airfoils.

MODELS AND APPARATUS

Small-Scale Rotor

Figure 2(a) is a photograph of the rotor which was 1.52 m (5.0 ft) in diameter and the 112-kW (150-hp) electric motor mounted on a test stand. The wood rotor blades (fig. 2(b)) had a constant 6.99 cm (2.75 in.) chord, a NACA 0012 airfoil section, and a 3° twist from root to tip (tip at smaller angle of attack than root). The leading-edge serrations and locations on the rotor blades are shown in figure 3. The serrations were cut out of brass by an electric discharge machine and were attached to the blades by small wood screws.

Large-Scale Rotor

Figure 4(a) is a photograph of the 2.59 m (8.5 ft) diameter rotor and the gear box for the 261-kW (350-hp) electric motor mounted on a test stand. The rotor axis was 3.4 m (11 ft) above the floor. The rotor blades had a constant 21.34-cm (8.4-in.) chord, a NACA 0015 airfoil section, and no twist. The blades were aluminum-skin-honeycomb construction. A close-up photograph (fig. 4(b)) shows a leading-edge serration mounted on the rotor. The various leading-edge serrations and locations on the rotor blade are shown in figures 5(a) and 5(b).

Microphone Stations

The acoustic data for the small-scale rotor test were taken with a hand-held microphone on a circle 4.57 m (15 ft) from the rotor center. The microphone was held in the horizontal plane intersecting the rotor hub. Figure 6 shows the microphone locations for the large-scale rotor test. The microphones were mounted on 1.83 m (6 ft) stands on a circle 7.62 m (25 ft) from the rotor center.

Acoustic Instrumentation

Condenser-type (B&K) microphones were used which were 1.27 cm (1/2 in.) in diameter. A combination sound level meter octave band analyzer (General Radio) was used to record the small-scale rotor noise. A 6 percent[1] bandwidth analyzer and graphic level recorder (B&K) were used to record the signals directly from the microphones during the large-scale rotor test (no tape recorder in system). Microphone cables of 30.5 to 39.6 m (100 to 130 ft) in length were used between the microphones with cathode followers and the graphic level recorder. The microphones numbered 6 and 7 (see fig. 6) had nose cone shields because of the rotor slipstream impinging on them. The data from microphone 7 were not as reliable as the other data because of wind effects. The data obtained from microphone 2 were erroneous and are not presented.

---

[1] Filter bandwidth equals 6 percent of center frequency.

All microphones were calibrated frequently using a pistonphone with an output of 124 dB at 250 Hz. Rotor noise measurement repeatability was found to be approximately ±1 dB.

Corrections

The 1.52-m (5.0-ft) data have been corrected for the effects of background noise for those cases where the background noise was within 10 dB of the measured rotor noise (ref. 7). The background noise was predominantly in the 63-Hz octave band. Some of the low rpm data were completely masked by background noise and are not presented. The 2.59 m (8.5 ft) rotor test background noise did not affect the data presented. No corrections were made for reverberations in the test area or ground reflections since these factors are believed to have had a negligible effect on changes in overall noise level due to changes of rotor parameters. However, the possibly substantial effect of ground reflections on the narrow band data was not determined.

TESTING AND PROCEDURE

Both rotors were operated in the shop of the Ames Large-Scale Aerodynamics Branch. The shop is approximately 27 m (90 ft) by 38 m (125 ft) in area and 38 m (125 ft) high with a concrete floor and corrugated fiberboard walls; it contained various amounts of machinery, large aircraft models, and support beams. The nearest obstacles to the larger rotor are shown in figure 6.

Small-Scale Rotor Test

While the rotor 1.52 m (5.0 ft) in diameter was being tested, the large shop doors (18 m (60 ft) wide by 9 m (30 ft) high) were open. The rotor was operated at various rotational speeds with constant blade angles of 4°, 8°, 10°, and 12°. A maximum speed of 1440 rpm (tip speed of 115 m/sec (377 ft/sec)) was imposed because of structural limits. The maximum chord-based Reynolds number at the tip was 550,000. The data were taken with a hand-held microphone 4.57 m (15 ft) from the rotor center. The rotor was operated with and without serrations on the blades. High rpm data were not obtained with the 0.76-cm (0.3-in.) serration on the rotor. Instrumentation for performance measurements were not available.

Large-Scale Rotor Test

Noise measurements were made of the 2.59 m (8.5 ft)-diameter rotor with the shop doors open and closed. The rotor rotational speed was varied from 500 rpm to 1600 rpm (maximum tip speed of 217 m/sec (711 ft/sec)) and the blade angles of attack were 6°, 12°, and 18°. The maximum chord-based Reynolds number at the tip was 3,180,000. Noise data were recorded by fixed microphones on a semicircle 7.62 m (25 ft) from the rotor center. Thrust and torque were measured using strain gages mounted on a nonrotating retainer hub. Electric motor power was monitored. Load cells for measuring thrust and torque were calibrated before and during the test. Some of the noise data corresponding to 500 rpm were masked by background noise and are not presented.

RESULTS

Small-Scale Rotor Test

The sound pressure levels around the small-scale rotor are shown in figure 7. Figures 8(a) through 8(d) show the effect of leading-edge serrations on the overall sound pressure level for different rotational speeds and blade angles. An octave band analysis of typical rotor noise with and without serrations on the leading-edges of the rotor is given in figure 9.

Large-Scale Rotor Noise

Figures 10 through 13 show the overall sound pressure levels measured around the rotor for various serration shapes and positions. The effect of serrations on the harmonics of blade passage frequency are shown in figures 14 through 17.

Performance data are presented in figures 18 and 19 as curves of thrust parameter C_T/σ versus torque parameter C_Q/σ and in figures 20(a) through 20(e) as curves of figure of merit versus C_T/σ.

DISCUSSION

Small-Scale Rotor

The small-scale rotor overall noise was consistently reduced 4 to 8 dB by the leading-edge serrations of figures 2(b) and 3 for all but the 4°-blade-angle condition (see figs. 8(a) through 8(d)). At the points labeled "rough" the rotor emitted a buzzing sound whose level varied ±2 dB every 5 to 10 seconds. The noise reductions due to serrations could be easily detected by ear as the loud, whistling noise from the clean rotor was replaced by a quieter, broad band sound from the serrated blades. The 1440 rpm rotational speed (115 m/sec (377 ft/sec) at the tip) corresponded to a tip Reynolds number of 550,000 based on the chord. Similar noise reductions by leading-edge serrations were observed by Hersh and Hayden (ref. 5) and by Arndt and Nagel (ref. 6).

The octave band frequency spectrum illustrated in figure 9 is typical for this rotor and indicates that the noise generated by the unserrated rotor was primarily high frequency. The peak in the noise spectrum at 8000 Hz was due to oscillating loads on the blades caused by shedding of a vortex street and was not due to rotational noise. This is based on results for similar flow conditions reported in references 5 and 8. It was the high frequency noise which was reduced by the serrations. Any noise reduction in the 31 Hz and 63 Hz octave bands may have been masked by background noise.

Large-Scale Rotor

Leading-edge serrations reduced the noise of the large-scale rotor less than for the small-scale rotor. Figures 10 through 13 illustrate the effect of serration shape, size, and location on the overall

noise levels. The largest noise reductions occurred at 800 and 1000 rpm, with little reduction at 1400 and 1600 rpm. Tip Reynolds numbers based on the chord were 1,590,000 at 800 rpm and 3,180,000 at 1600 rpm. It was not possible to obtain rotor noise data at lower Reynolds numbers because the sound generated by the rotor at lower rotational speeds was masked by the background noise.

Effect of serration size and location on the overall noise level– Tables 1 and 2 summarize the effects of serrations 1, 3, 4, and 5 for a rotational speed of 800 rpm, the speed at which the serrations were most effective at reducing noise. Serrations 3 and 4 reduced the overall noise levels up to 4 dB as shown in table 1. For most conditions, serrations 3 and 4 gave better results than serration 5, the largest serration tested. Serration 1, which had no spacing between prongs (see fig. 5(a)), did not perform as well as the others. Therefore, these limited data suggest that the smaller serrations (0.13 to 0.25 cm (0.05 to 0.10 in.)) with gaps between prongs reduced the noise more effectively than did the larger serration (0.64 cm (0.25 in.)) and the serration without gaps.

Tables 1 and 2 show that the positions of serrations 3 and 5 on the rotor blade had a large effect on noise reduction. At an 18°-blade-pitch angle, moving the serration aft to position 3 was beneficial. At 12°, position 2 gave the largest noise reduction in most cases. This observation suggests that proper serration location depends on the stagnation point location. However, figures 10(d), 10(e), 11(c), 11(d), and 12(b) show that position 2 was a good compromise for all blade angles and rotational speeds tested.

Narrow band analysis– Narrow band frequency analyses of the large-scale rotor noise indicated that the peaks occurring at harmonics of the blade passage frequency, f_1, stood above the broad band noise. These peaks were relatively high for the first few harmonics since rotational noise was the major source. Under most conditions the peaks were above the broad band noise to the 10th harmonic in the 6 percent bandwidth spectrum plots.

Figures 14(a) through 14(c) show the noise levels at harmonics of the blade passage frequency for the rotor with and without serration 3 as measured with microphone 5. The overall noise levels were dominated by the noise in the 1st harmonic of blade passage frequency. Therefore, noise reductions in overall noise were due to reductions in noise at the blade passage frequency and not due to reductions in higher frequency noise. At 1000 rpm and at blade angles of 6°, 12°, and 18°, the noise in harmonics 3 through 8 were generally lower for serration 3. This observation suggests that the serration was reducing oscillating blade pressures associated with periodic blade loading. This reduction did not occur at 1400 rpm.

Figures 15(a) through 15(c) show little noise reduction due to serration 5 except at 1000 rpm, and $\beta = 18°$, when higher frequency noise was reduced.

The only acoustic data taken at 500 rpm are presented in figure 16. At this lower tip Reynolds number (993,000), serration 2 in position 3 reduced the vortex noise up to 10 dB. The tip speed for this condition was the same as that for the small-scale rotor at 840 rpm, which resulted in a 8.5 dB noise reduction due to serrations. This indicates that serrations perform the best at low Reynolds numbers where higher harmonics of rotational noise and the noise generated by vortex shedding are a greater component of the generated noise.

TABLE 1.– MAXIMUM NOISE REDUCTION, ΔdB, AT 800 RPM

Blade angle	$\beta = 6°$			$\beta = 12°$			$\beta = 18°$		
Position[a]	1	2	3	1	2	3	1	2	3
Serration 1[a]	–	–	–	–	1.0	–	–	–	–
Serration 3	2.0	–	–	2.0	1.5	2.0	−2.5[b]	–	4.0
Serration 4	–	–	–	–	–	–	4.0	3.0	4.0
Serration 5	–	–	–	−2.0	3.0	0.5	−2.5	3.0	2.0

[a]Figure 5 illustrates position and serration number.

[b]Numbers with negative sign are maximum noise increase. Dashes indicate that no data are available.

TABLE 2.– AVERAGE NOISE REDUCTION, ΔdB[a], AT 800 RPM

Blade angle	$\beta = 6°$			$\beta = 12°$			$\beta = 18°$		
Position	1	2	3	1	2	3	1	2	3
Serration 1	–	–	–	–	0.3	–	–	–	–
Serration 3	1.5	–	–	0.8	1.0	1.0	−1.3[b]	–	3.0
Serration 4	–	–	–	–	–	–	2.0	0.4	2.0
Serration 5	–	–	–	−1.0	–	0	−2.0	0.2	1.4

[a]$\Delta dB = \sum_{i=1}^{5} \frac{\Delta dB_i}{5}$, where ΔdB_i is noise reduction at microphone i microphones 2 and 7 excluded.

[b]Numbers with negative sign are average noise increase. Dashes indicate that no data are available.

The complete 6 percent bandwidth frequency spectrums of the rotor noise are shown in figures 17(a) and 17(b) for the unserrated and serrated blades. These are typical of the frequency spectrums from which figures 14 through 16 were taken.

Effect of serrations on performance– Thrust and torque measurements showed that serrations did not adversely affect rotor performance. Figures 18(a) through 18(f) are plots of C_T/σ versus C_Q/σ for serration 3 at different positions and for various rotational speeds. The data show that rotor thrust could be maintained with serrations on the blades by increasing blade angle but without an increase in torque. Therefore, thrust could be maintained without an increase of power required. Figures 19(a) and 19(b) indicate that serration 5 did not affect the rotor performance.

Figure of merit is a measure of hover efficiency. Figures 20(a) through 20(e) represent typical data and show that rotor figure of merit was not degraded by adding serrations to the blades.

These performance measurements agree generally with results of an aerodynamic study (ref. 4) which showed that properly designed serrations did not degrade the performance of a two-dimensional airfoil in a wind tunnel. In fact, certain serrations increased maximum lift and angle of attack for maximum lift of the model. That effect was caused by vortices from the serrations which reduced separated flow on the airfoil upper surface.

CONCLUDING REMARKS

Noise level reductions from 4 to 8 dB overall sound pressure level and from 3 to 17 dB in the higher frequency octave bands were achieved with 0.25-cm (0.1-in.) serrated brass strips attached to the small-scale rotor leading edge. Noise reductions were obtained for rotational speeds of 600 to 1440 rpm (maximum speed tested) and blade angles of 8°, 10°, and 12°.

Serrations were less successful in reducing noise levels of the large-scale rotor. Serrations 3 and 4 in the most aft position on the blade leading-edge region reduced the overall sound pressure level up to 4 dB. Optimum serration position depended on stagnation point location, but position 2 was a reasonable compromise for all blade angles tested. Smaller serrations (0.13 to 0.25 cm (0.05 to 0.10 in.)) reduced the noise more effectively than did the larger serration (0.64 cm (.25 in.)).

The serrations were much more effective as noise suppressors at low tip speeds (48 m/sec (157 ft/sec) to 135 m/sec (444 ft/sec)) than at high tip speeds (190 m/sec (621 ft/sec) to 217 m/sec (710 ft/sec)). In terms of chord-based Reynolds numbers, the serrations were most effective at conditions corresponding to tip Reynolds numbers of 1,999,000 and lower. At high tip speeds, the rotor noise was dominated by low frequency rotational noise which was relatively unaffected by the serrations. At low tip speeds, the higher frequency noise was a significant part of the overall noise and was reduced by the serrations. This high frequency noise included the sound generated by vortex shedding and, in the case of the large-scale rotor, the higher harmonics of rotational noise.

Serrations did not appreciably affect performance of the large-scale rotor (the small rotor wasn't instrumented). Thrust levels could be maintained for a given input power with serrations on the rotor.

An explanation of the noise reduction mechanisms of leading-edge serrations is reported in reference 5. That study shows that leading-edge serrations generate vortices on the airfoil upper surface and generate a turbulent boundary layer on the lower surface. This effect reduces separated flow regions and also eliminates periodic fluctuations in the wake such as those caused by vortex streets. Fluctuating blade loads and generated noise are thereby reduced. A similar study (ref. 6) indicated that serrations generate small-scale vortices which serve to break up rotor tip vortices.

Ames Research Center
National Aeronautics and Space Administration
Moffett Field, Calif., 94035, November, 1972

REFERENCES

1. Graham, R. R.: The Silent Flight of Owls. J. Roy. Aeron. Soc., vol. 38, 1934, pp. 837–843.

2. Hertel, Heinrich: Quiet Flying – Damping Flight Noise. Structure – Form – Movement, ch. B, sec. 11, M. Katz, transl. ed., Reinhold Pub. Corp. (New York), 1966, pp. 16–19.

3. Hickey, David H.: Some Developments in the Noise Reduction in Ducted Propellers and Fans. Conf. on STOL Transport Aircraft Noise Certification, Wash., D. C., FAA–NO–69–1, Jan. 30, 1969, pp. 104–118.

4. Soderman, Paul T.: Aerodynamic Effects of Leading-Edge Serrations on a Two-Dimensional Airfoil. NASA TM X–2643, 1972.

5. Hersh, Alan S.; and Hayden, Richard E.: Aerodynamic Sound Radiation from Lifting Surfaces With and Without Leading-Edge Serrations. NASA CR–114370, 1971.

6. Arndt, Roger E.; and Nagel, Robert T.: Effect of Leading Edge Serrations on Noise Radiation from a Model Rotor. AIAA Paper No. 72–655, 1972.

7. Peterson, Arnold P.; and Gross, Ervin E., Jr.: Effect of Background Noise in Handbook of Noise Measurement. Gen. Radio Co., Concord, Mass., 1967 (6th Edition), pp. 133–134.

8. Paterson, R. W.; Vogt, P. G.; Fink, M. R.; and Munch, C. L.: Vortex Shedding Noise of an Isolated Airfoil. Durham Report K910867–6, U.S. Army Research Office, Dec. 1971.

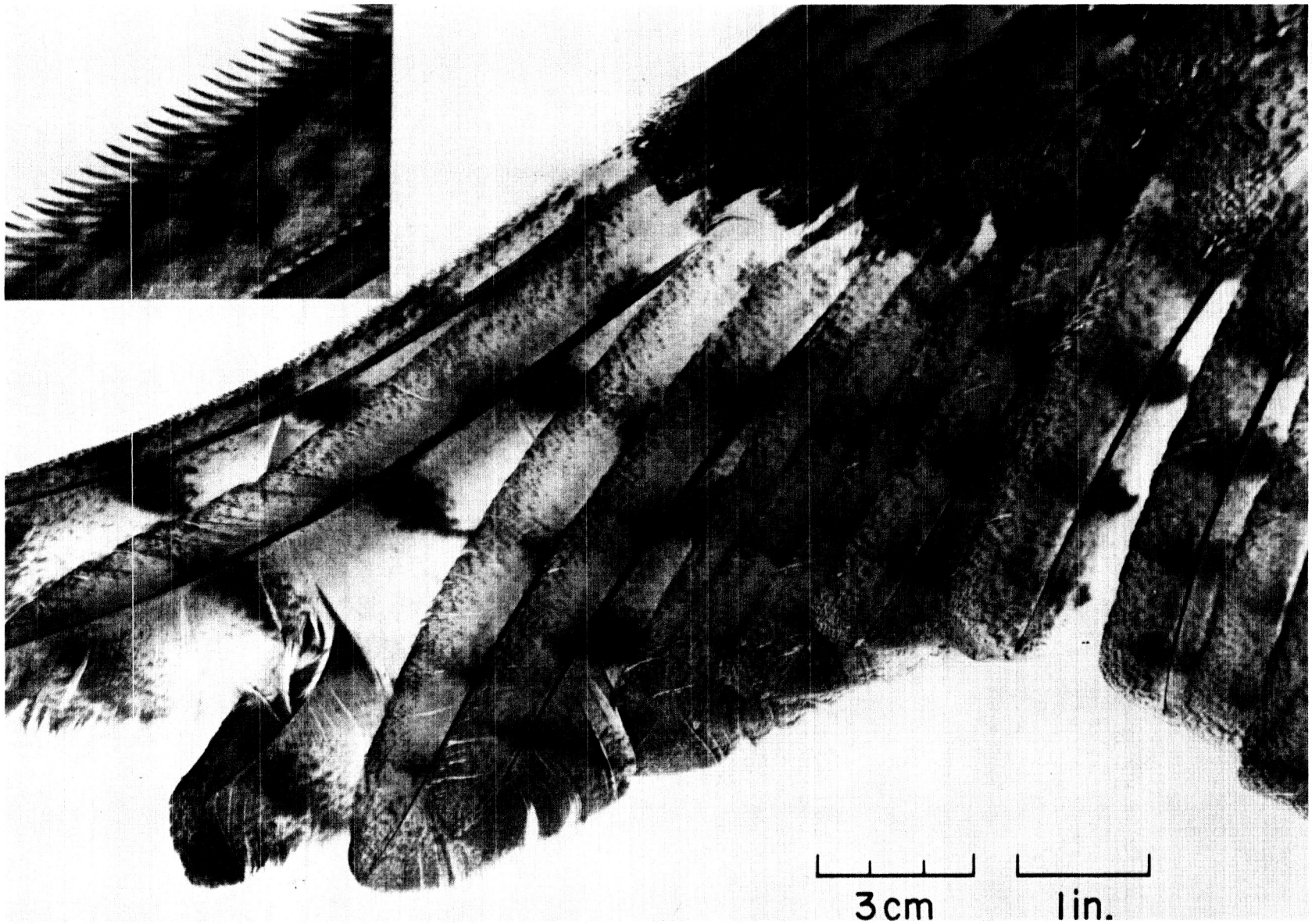

Figure 1.– Owl wing with leading-edge serrated feather.

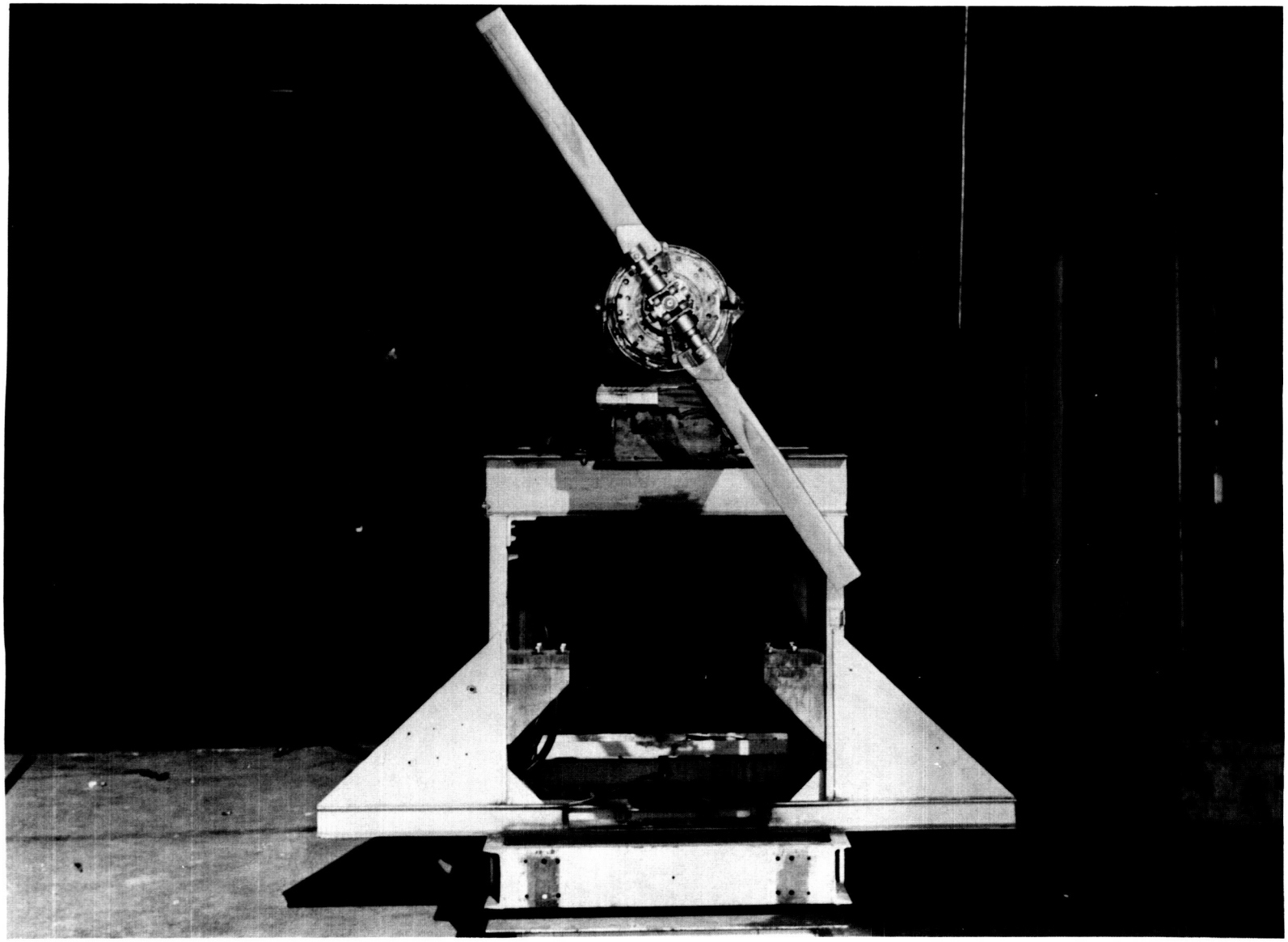

(a) Rotor and electric motor on test stand.

Figure 2.– Small-scale rotor model.

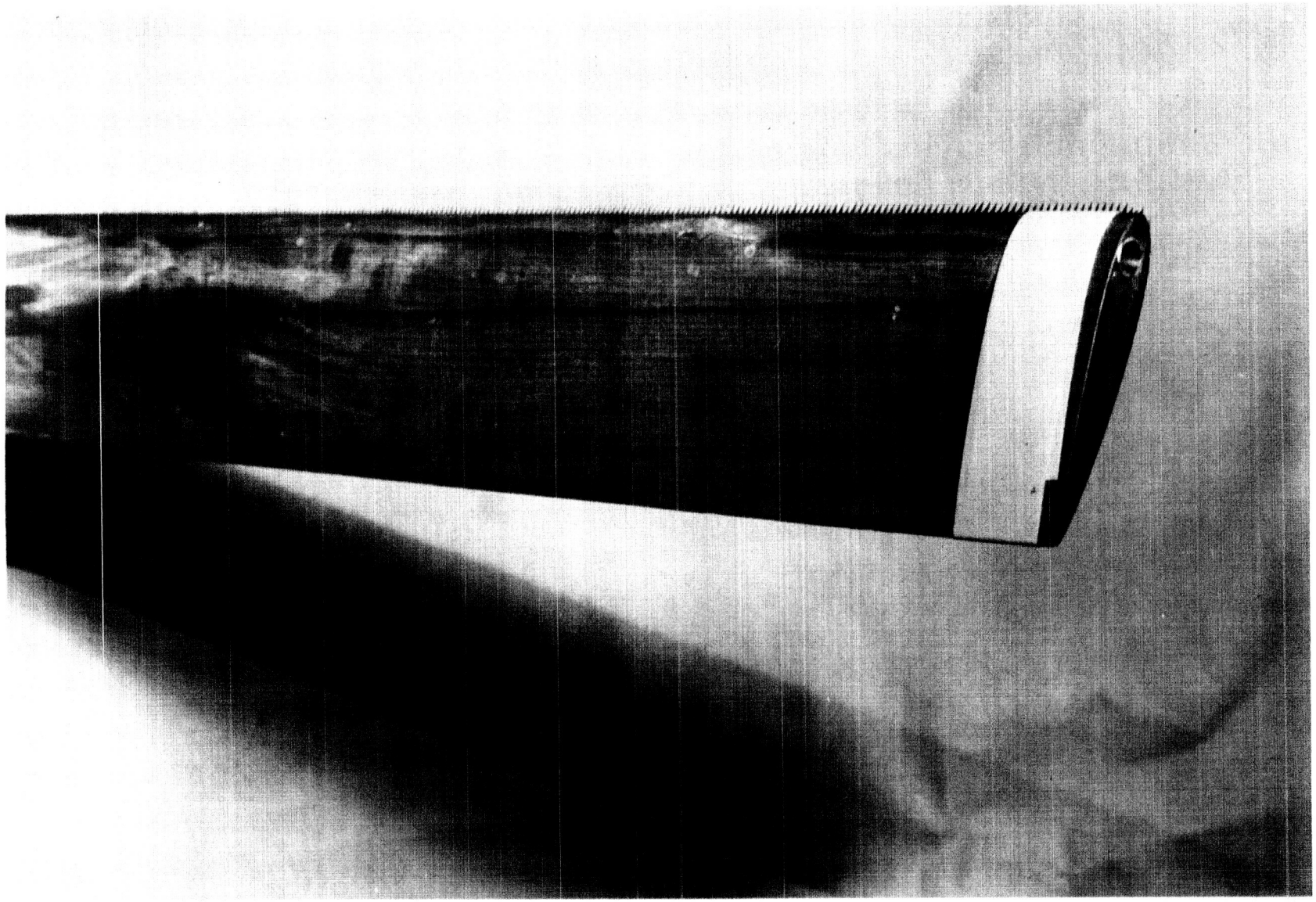

(b) Rotor blade with 0.25 cm (0.1 in.) serration.

Figure 2.– Concluded.

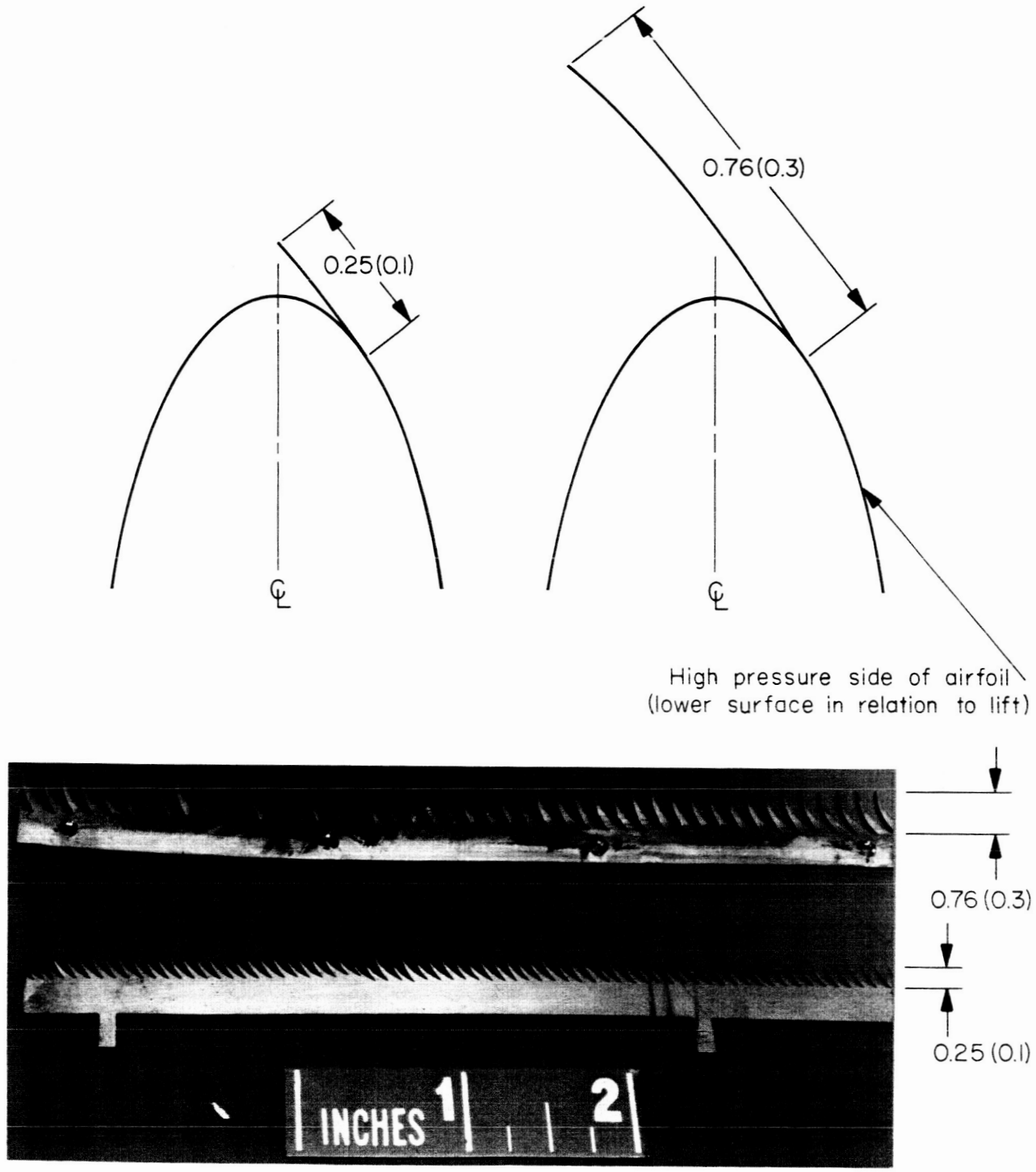

Dimensions in cm (in)

Figure 3.– Leading-edge serration position on small-scale rotor blade (top) and serration shape (bottom).

(a) Rotor and electric motor on test stand.

Figure 4.– Large-scale rotor model.

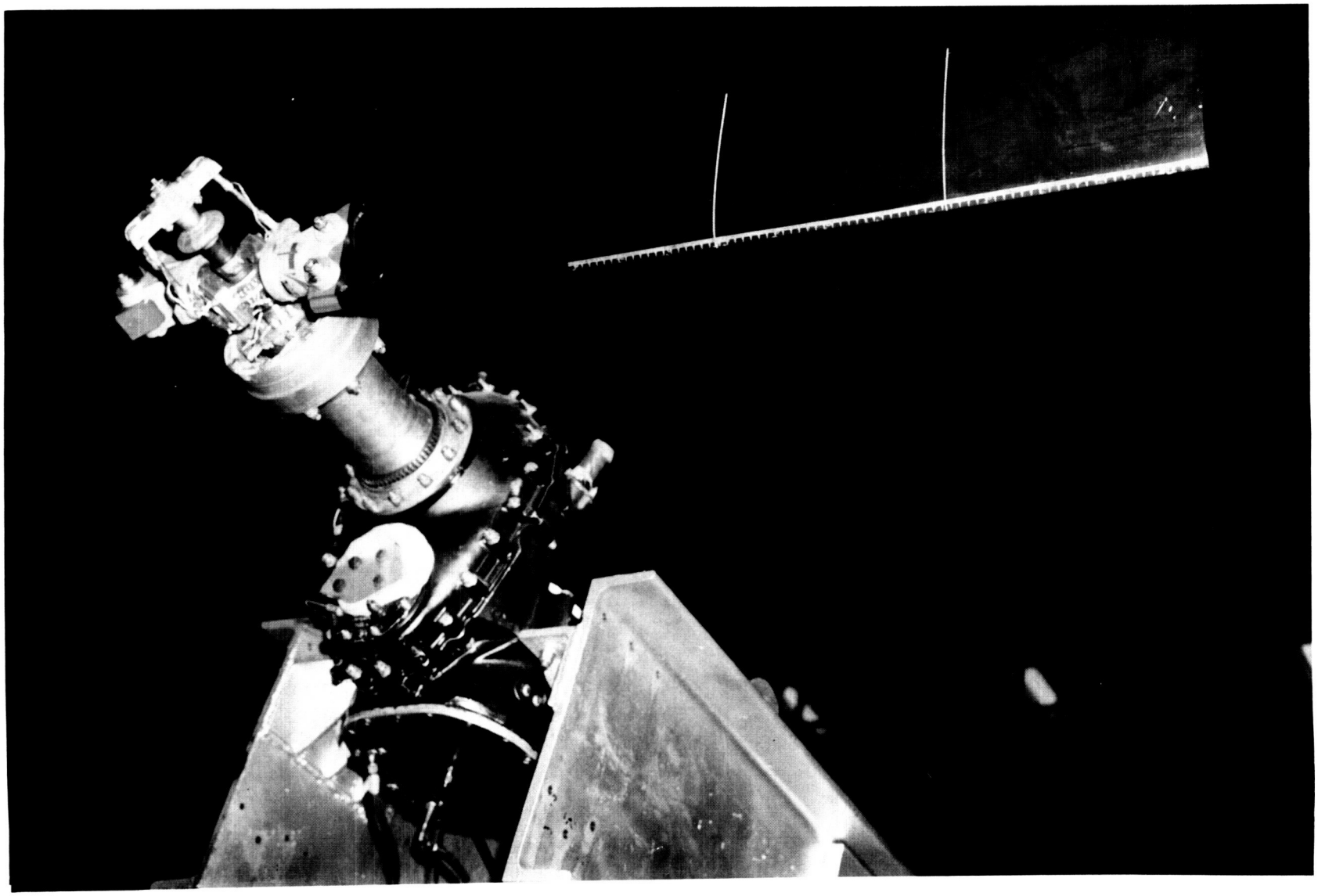

(b) Serration mounted on rotor leading edge.

Figure 4.– Concluded.

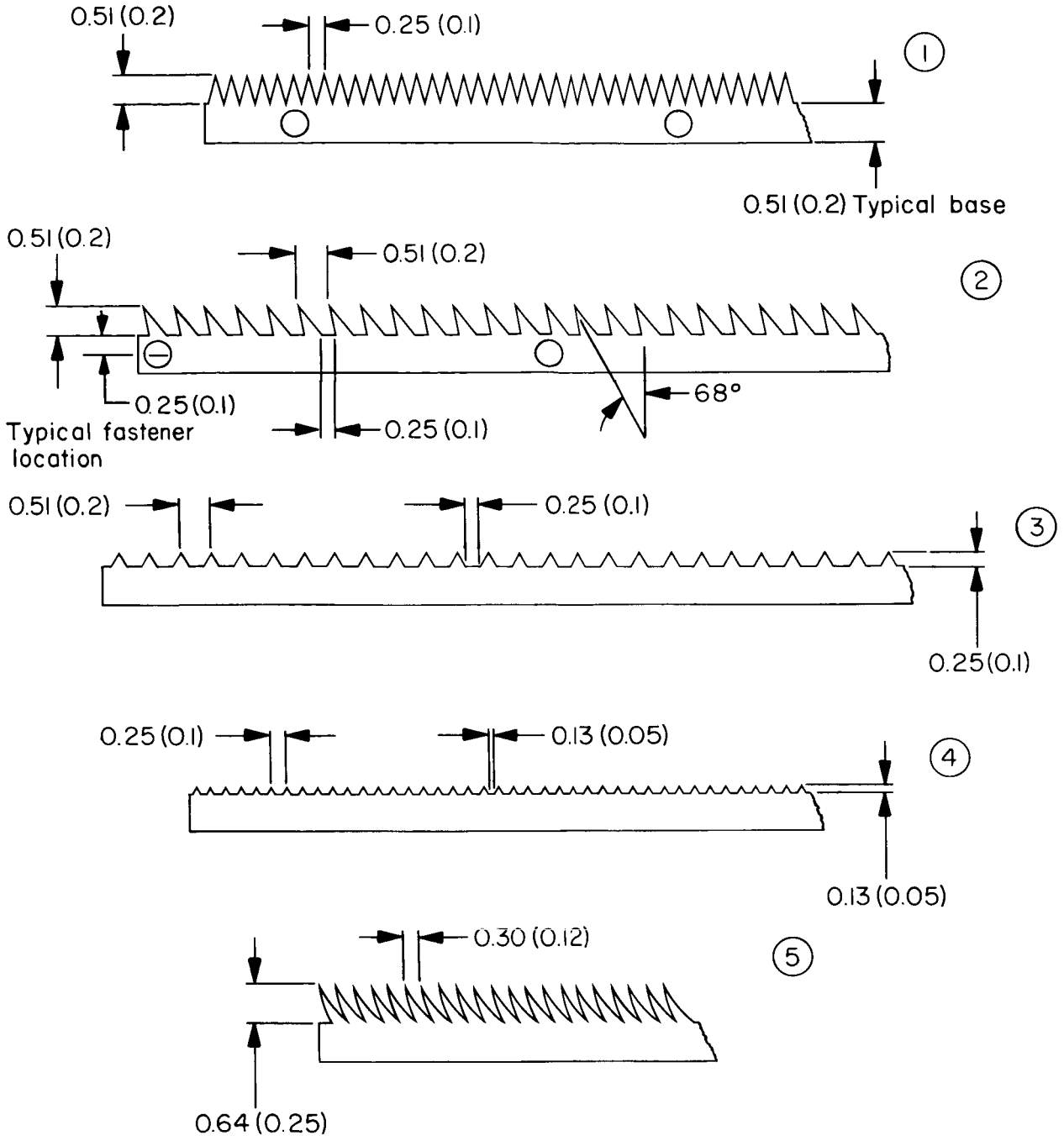

(a) General shapes and sizes.

Figure 5.– Serrations used on large-scale rotor.

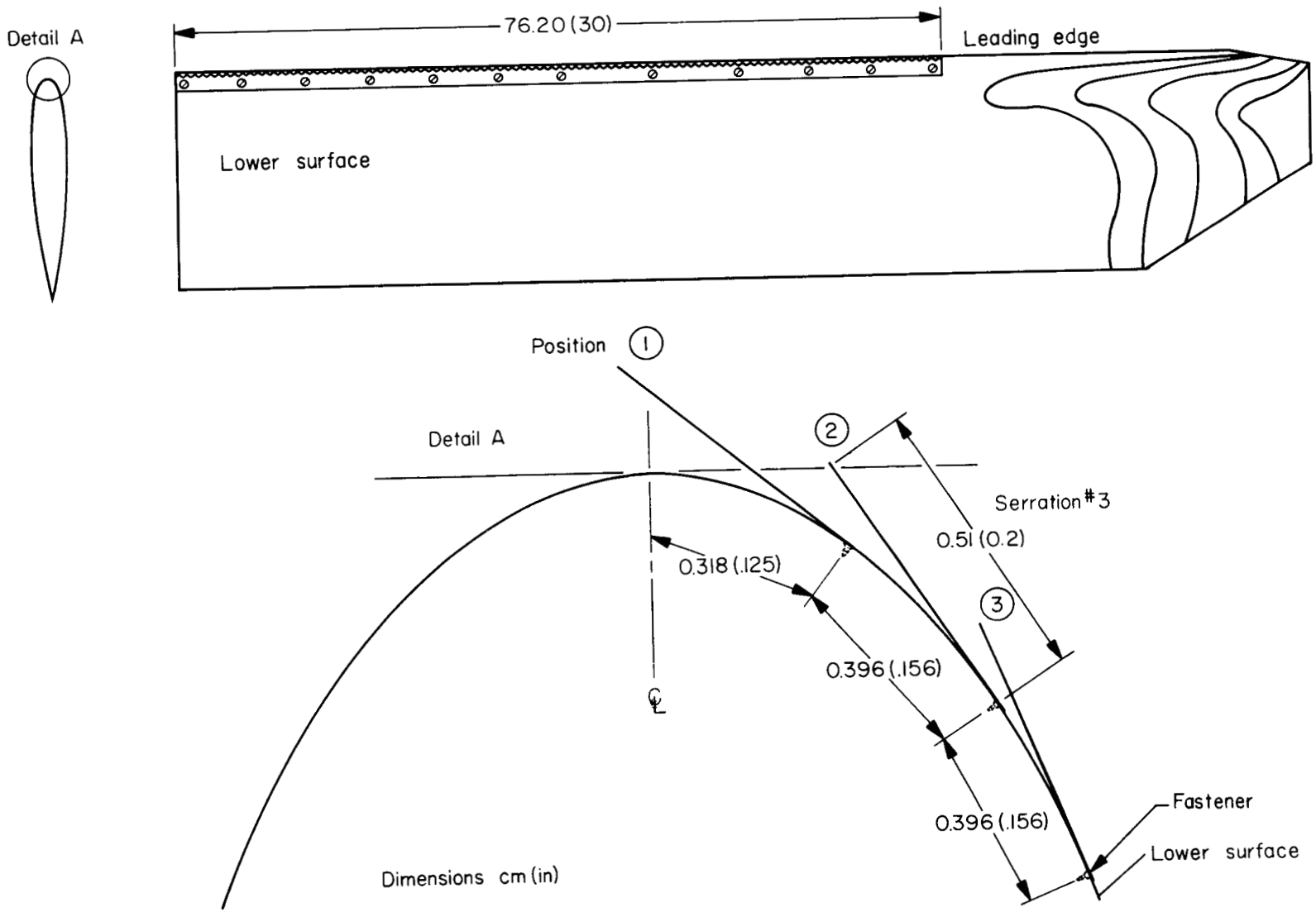

(b) Serration location on blade; fastener locations were unchanged for all serrations.

Figure 5.– Concluded.

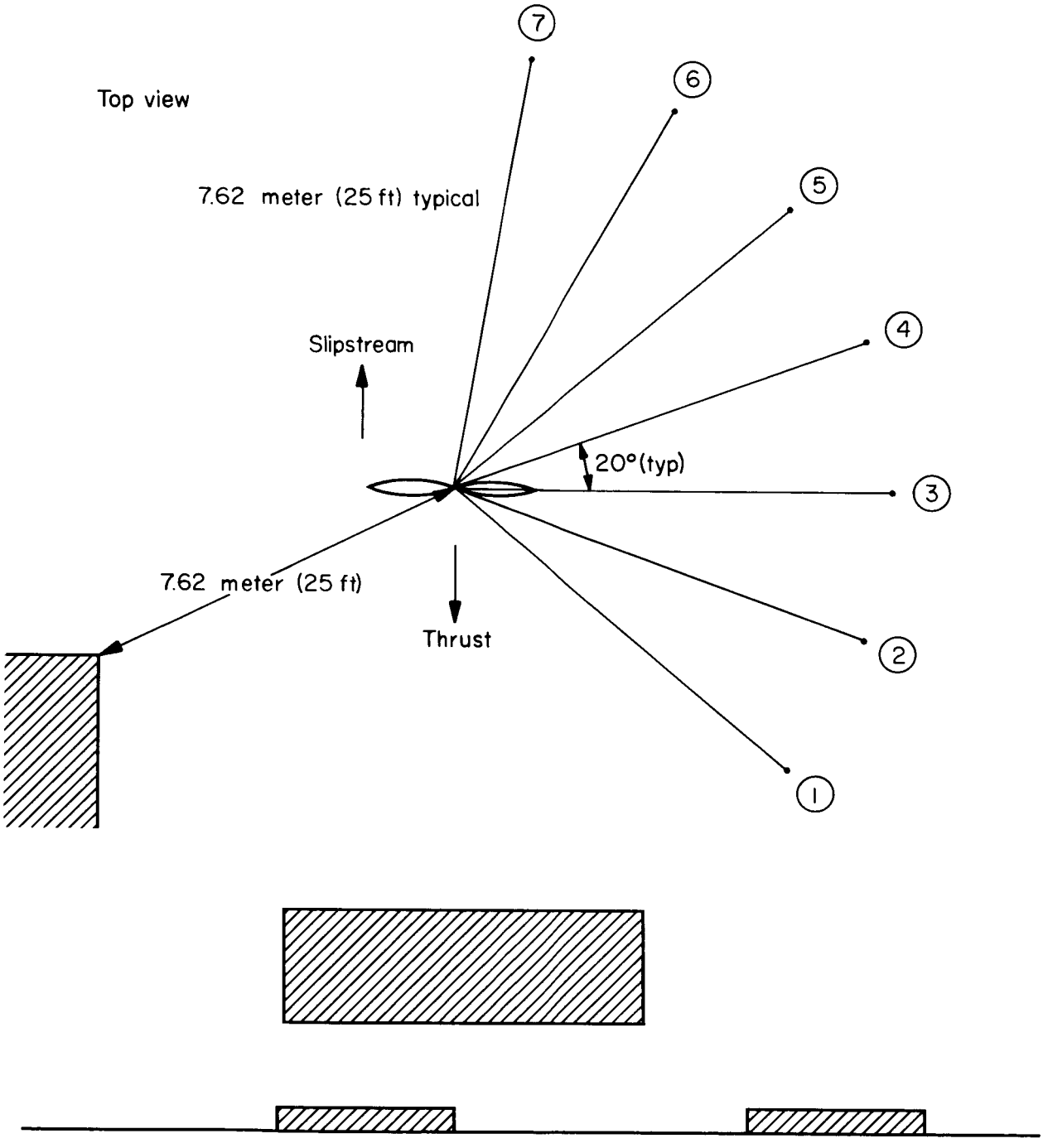

Figure 6.– Microphone locations relative to the large-scale rotor.

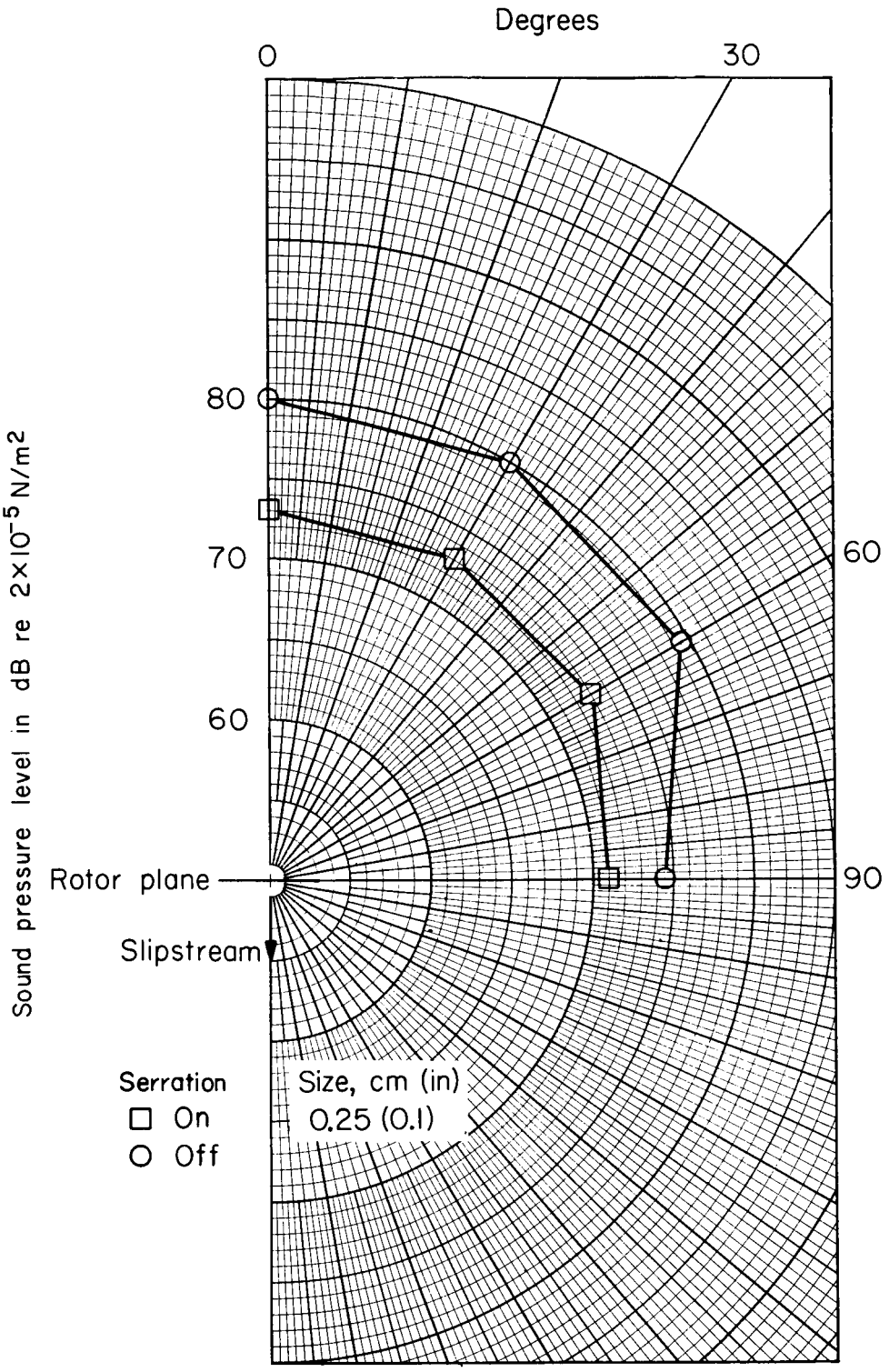

Figure 7.– Overall sound pressure levels at 4.6 m (15 ft) from the small-scale rotor, with and without serrations; $\beta = 8°$, $N = 1200$ rpm.

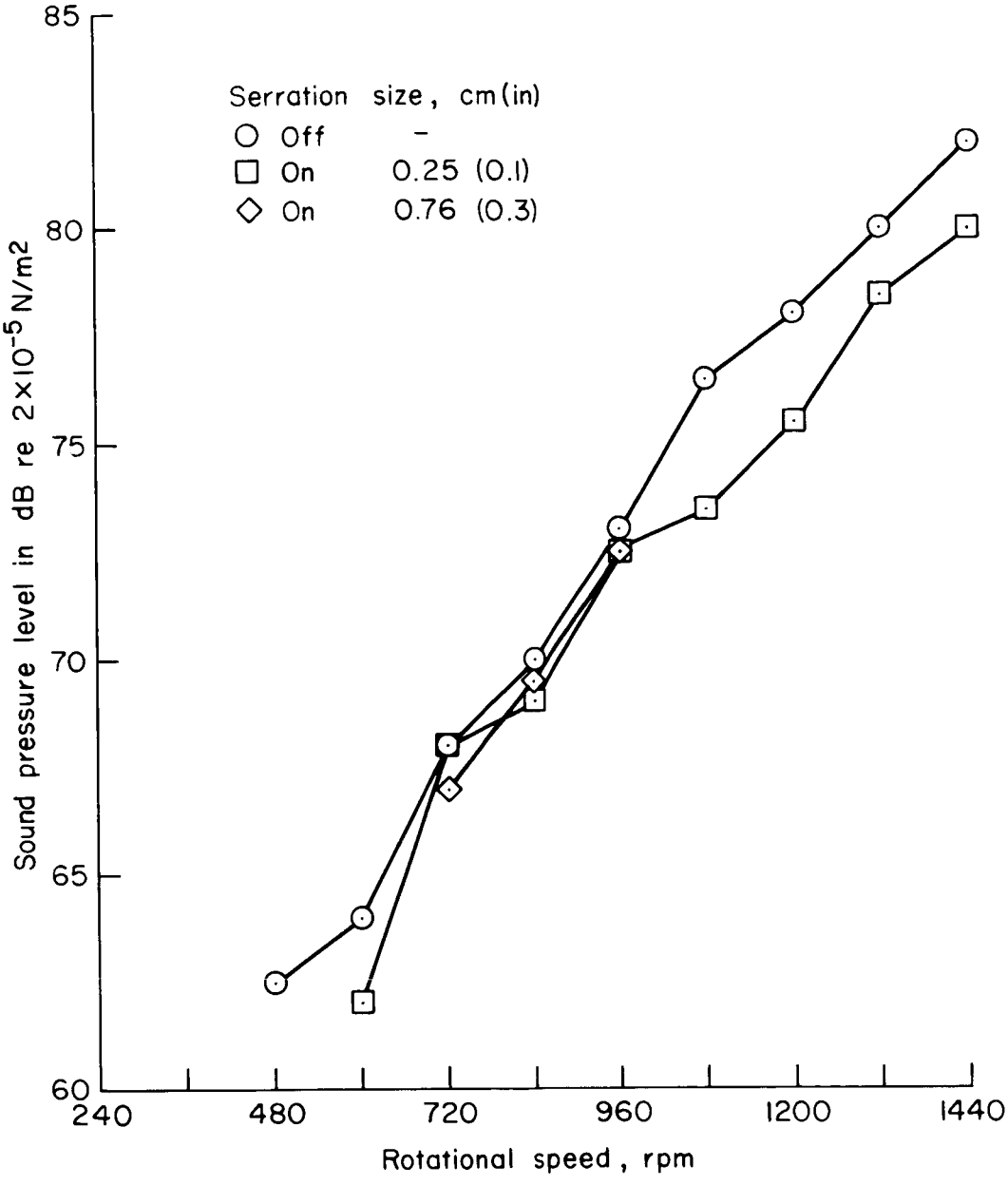

(a) $\beta = 4°$

Figure 8.– Overall sound pressure levels at 4.6 m (15 ft) from the small-scale rotor, with and without serrations, 0° from rotor axis.

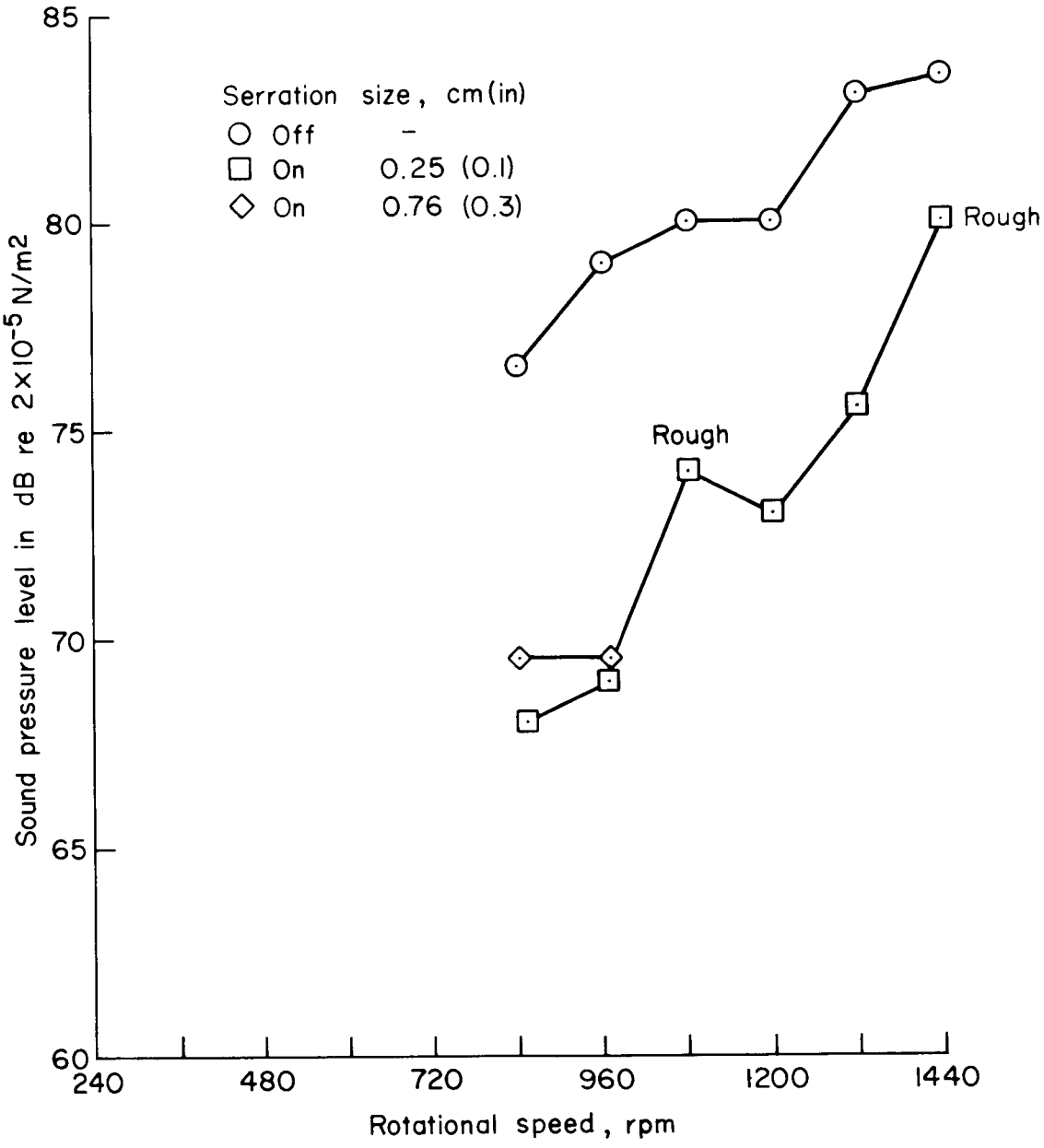

(b) $\beta = 8°$

Figure 8.– Continued.

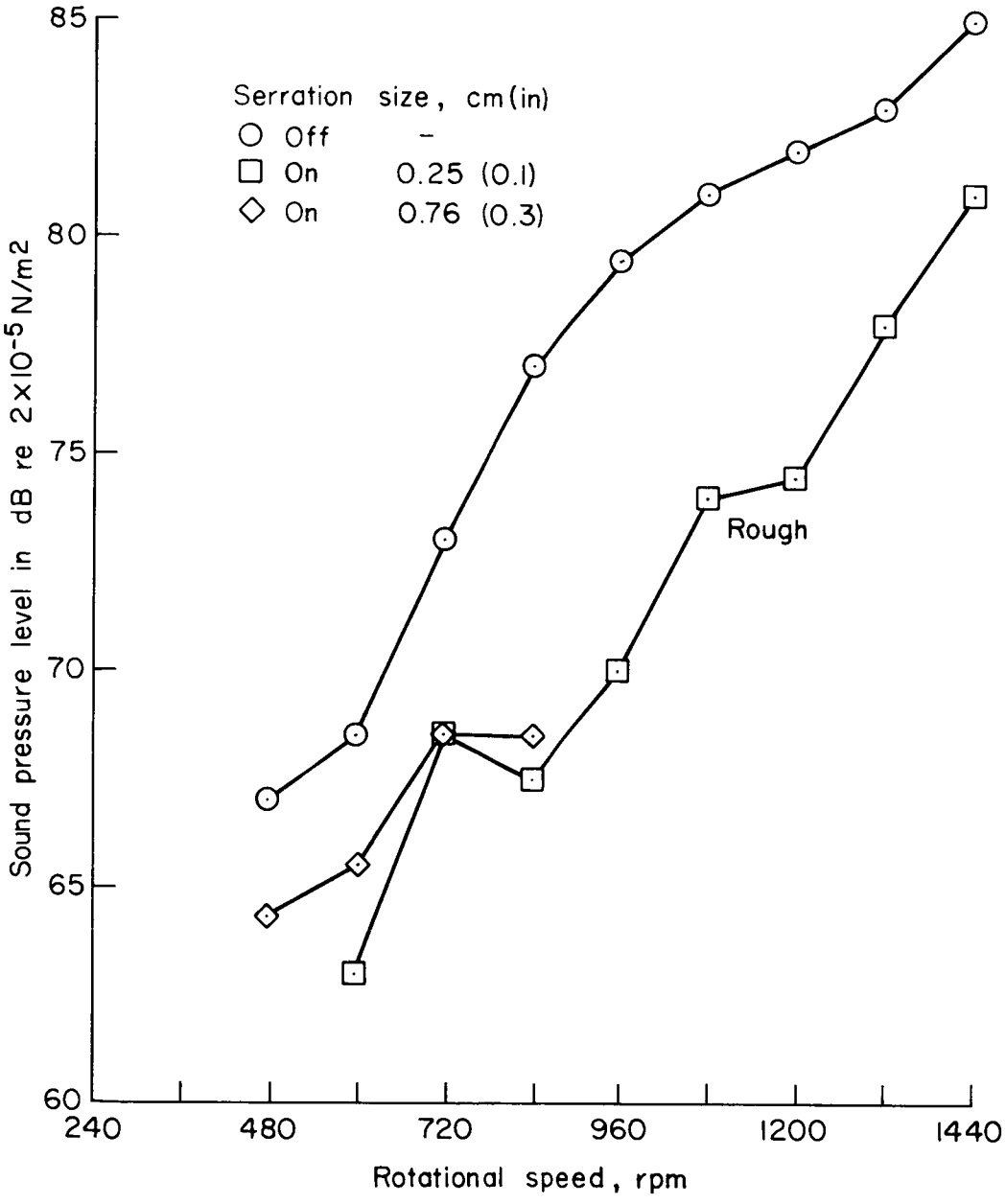

(c) $\beta = 10°$

Figure 8– Continued.

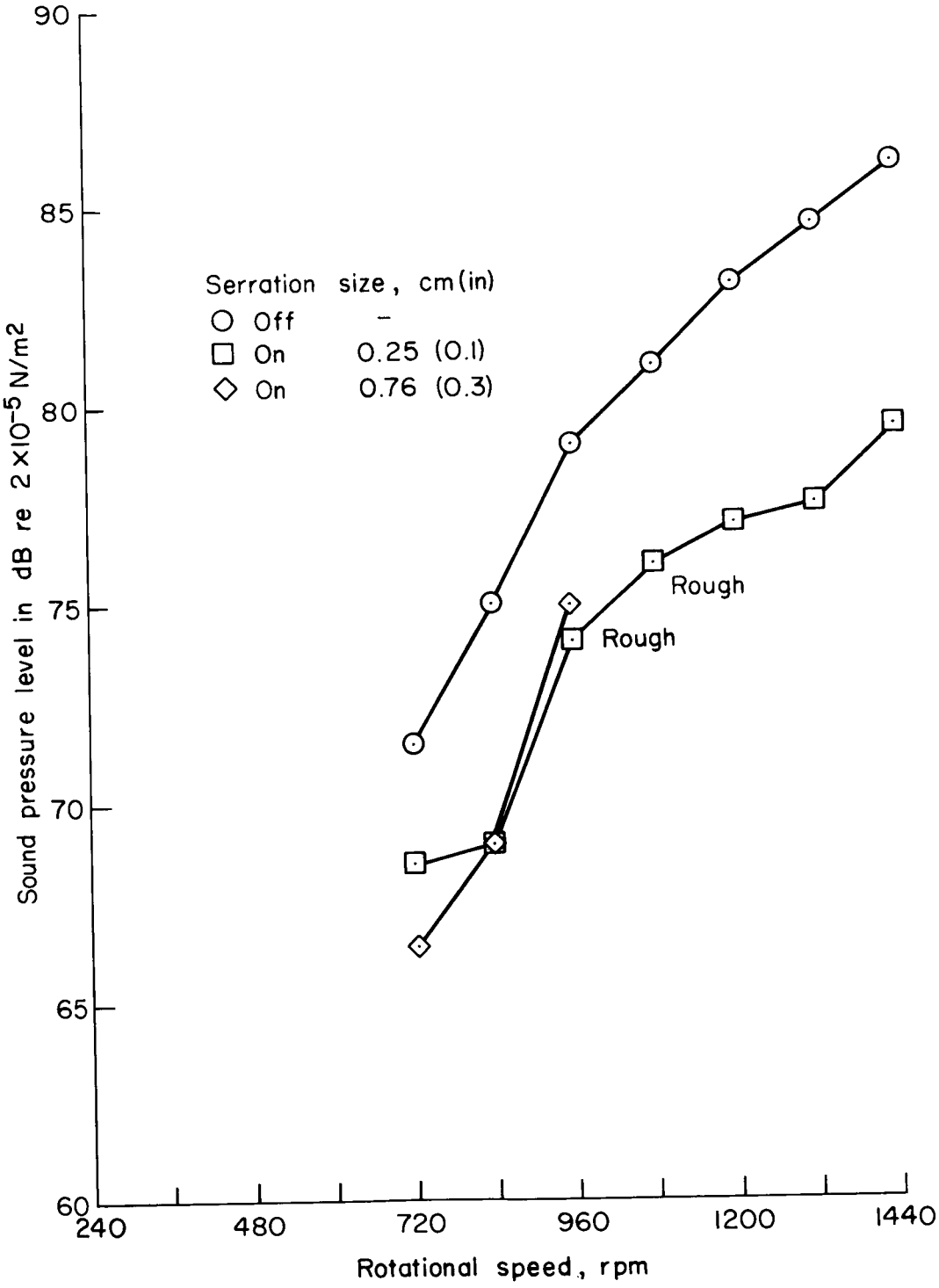

(d) $\beta = 12°$

Figure 8.– Concluded.

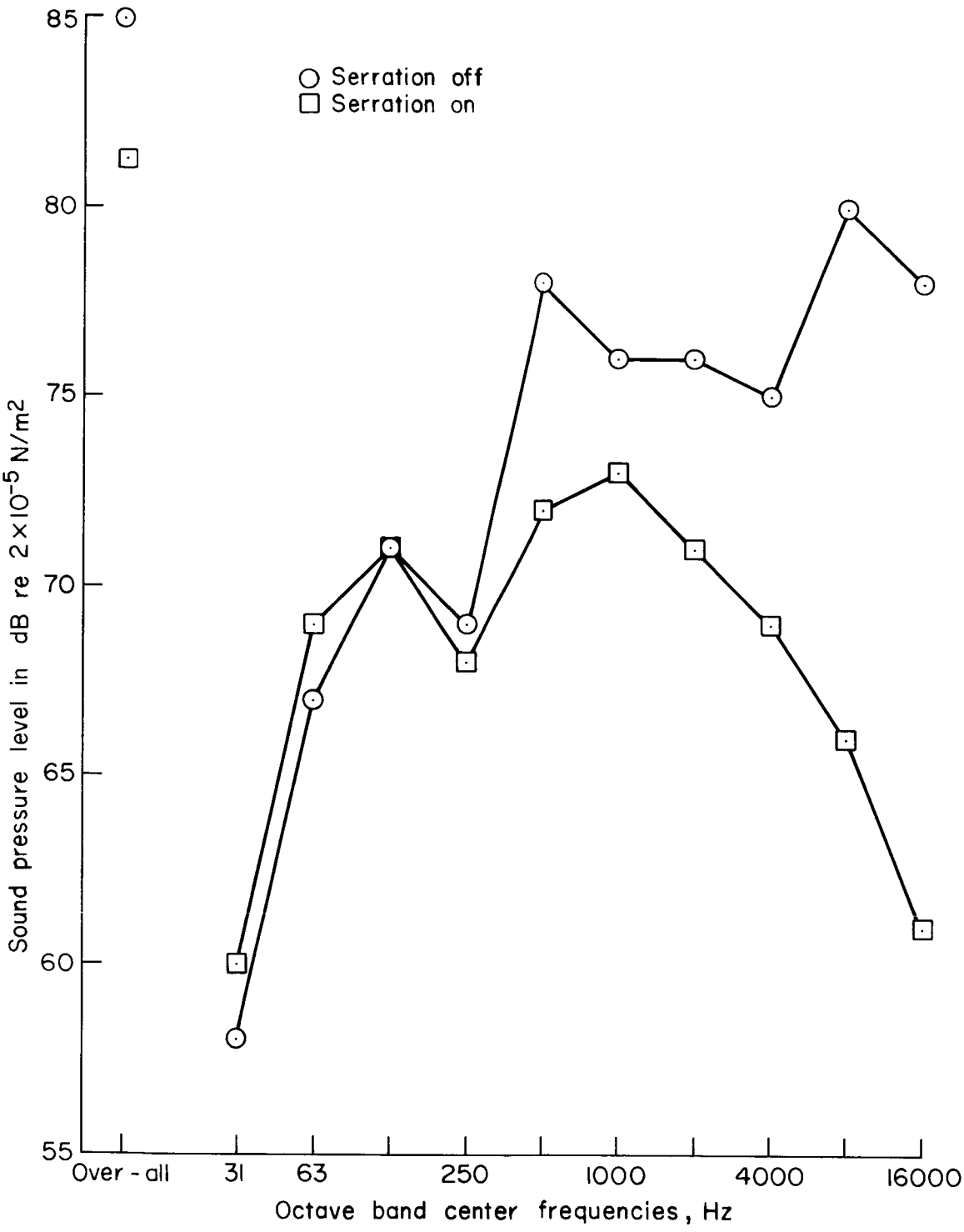

Figure 9.– Overall and octave band noise levels at 4.6 m (15 ft) from the small-scale rotor, with and without 0.25 cm serrations, 0° from rotor axis; $\beta = 10°$, $N = 1440$ rpm, tip speed = 115 m/sec (377 ft/sec), blade passage frequency = 48 Hz (63 Hz band).

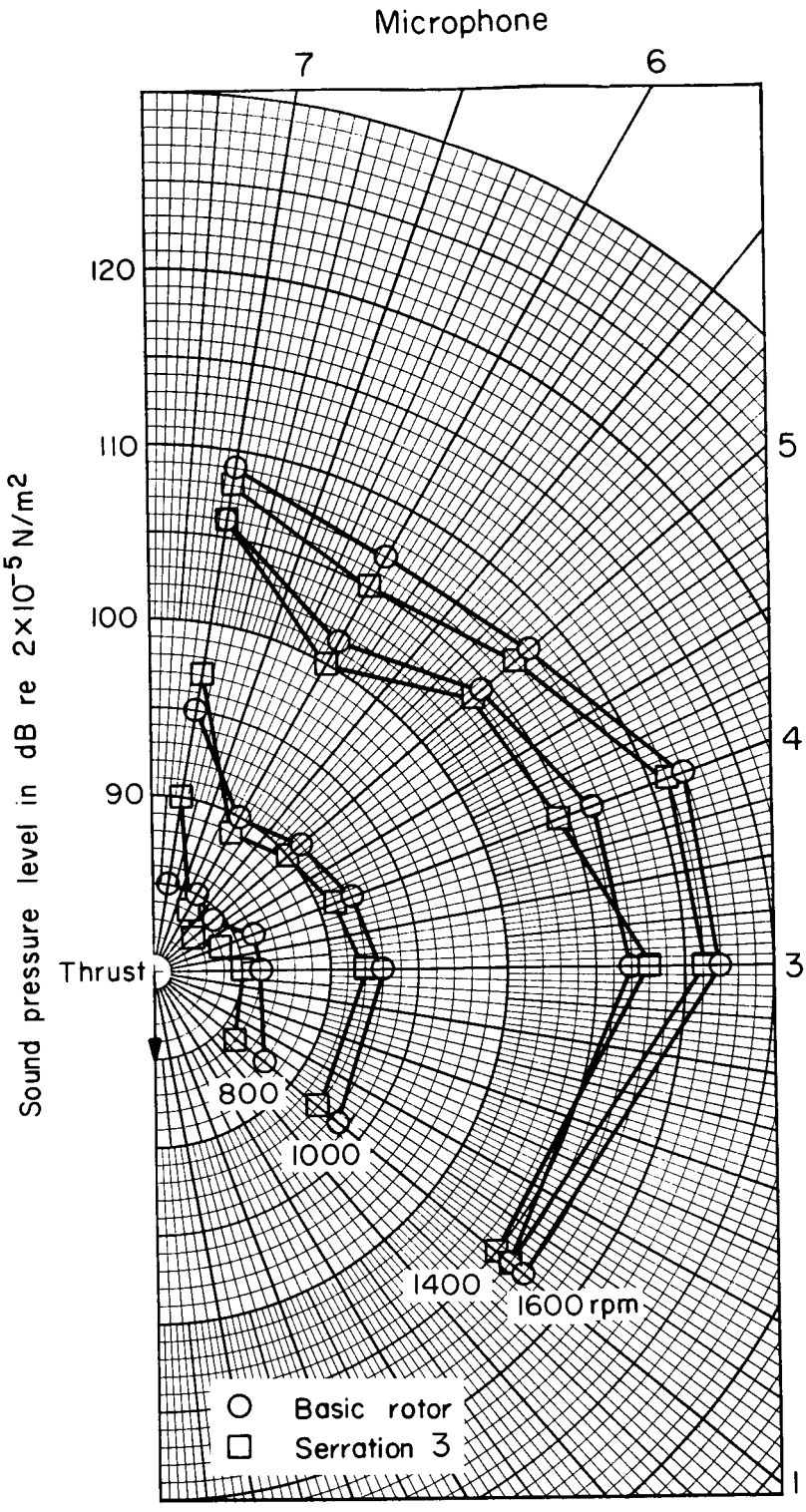

(a) Position 1, $\beta = 6°$.

Figure 10.– Overall sound pressure levels at 7.6 m (25 ft) from the large-scale rotor, with and without serration 3.

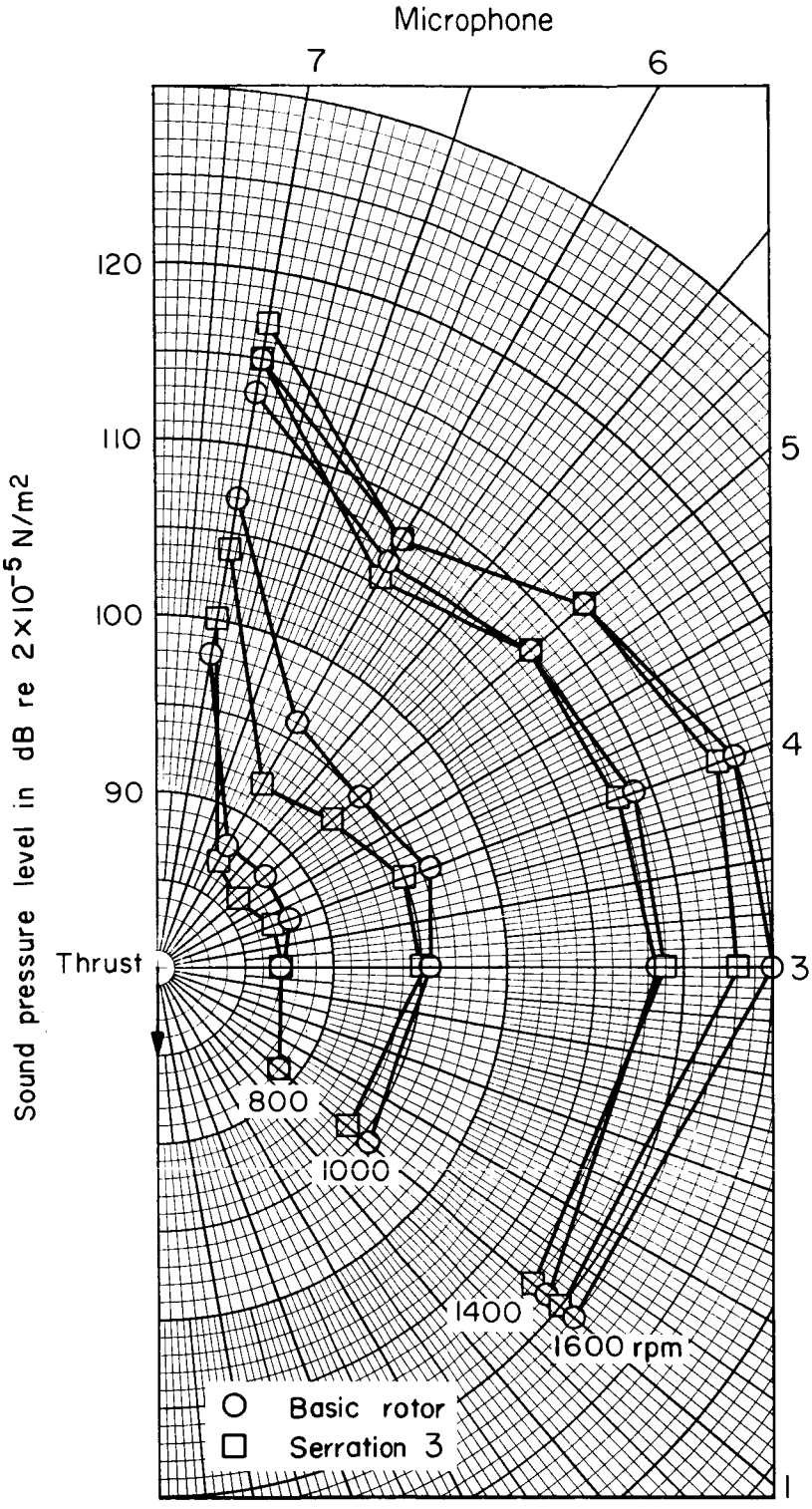

(b) Position 1, $\beta = 12°$.

Figure 10.– Continued.

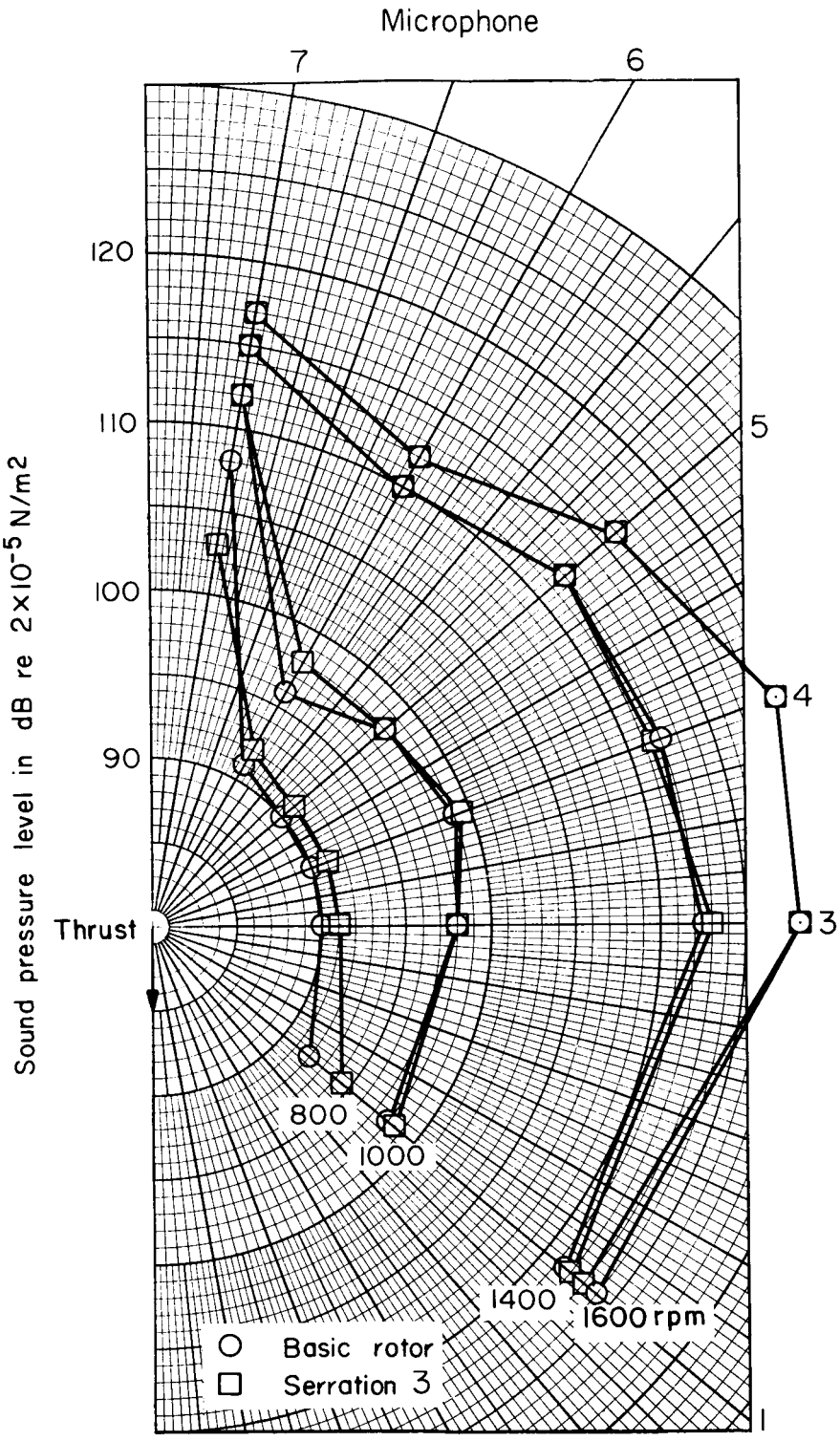

(c) Position 1, $\beta = 18°$.

Figure 10.– Continued.

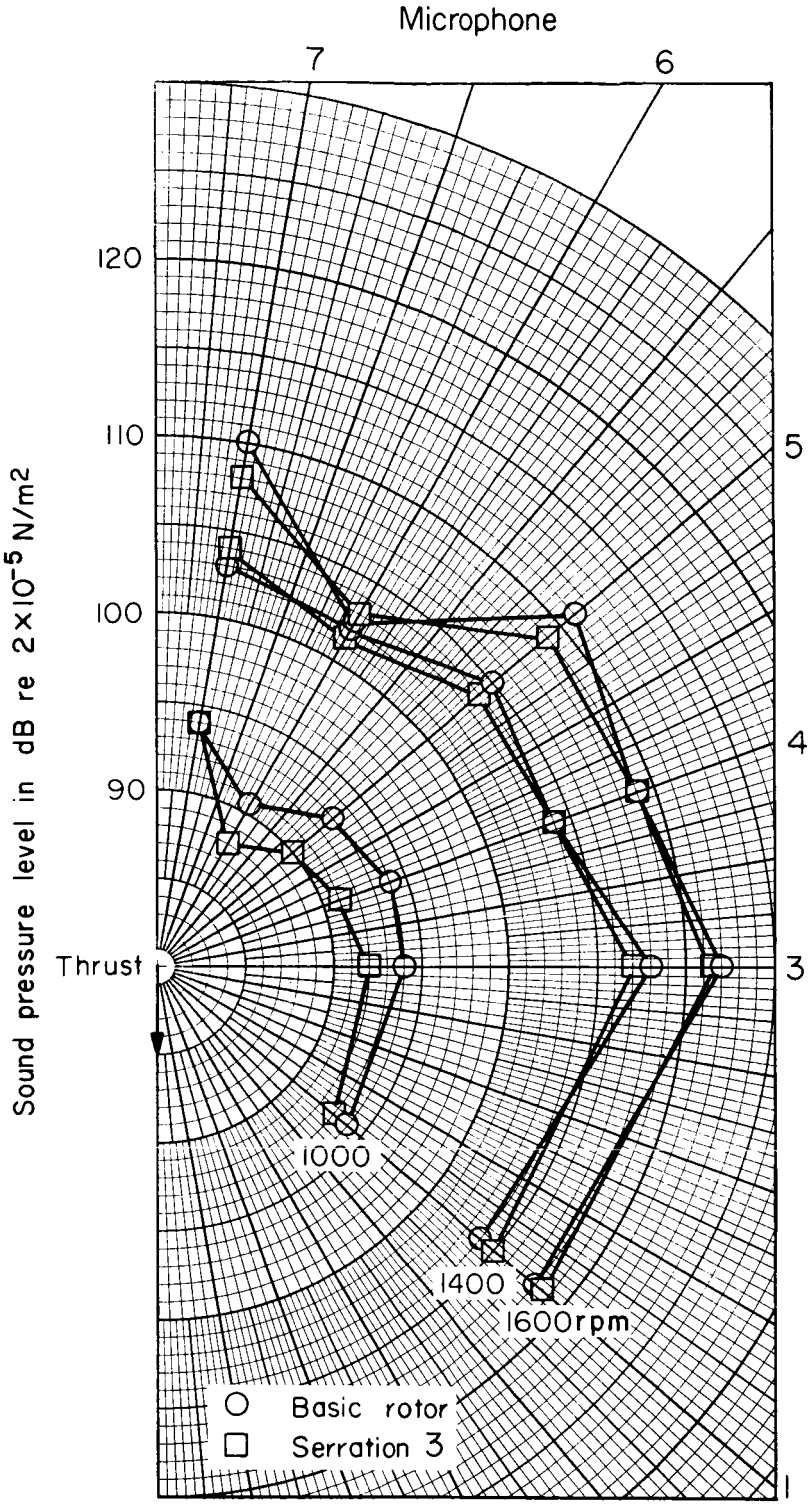

(d) Position 2, $\beta = 6°$.

Figure 10.– Continued.

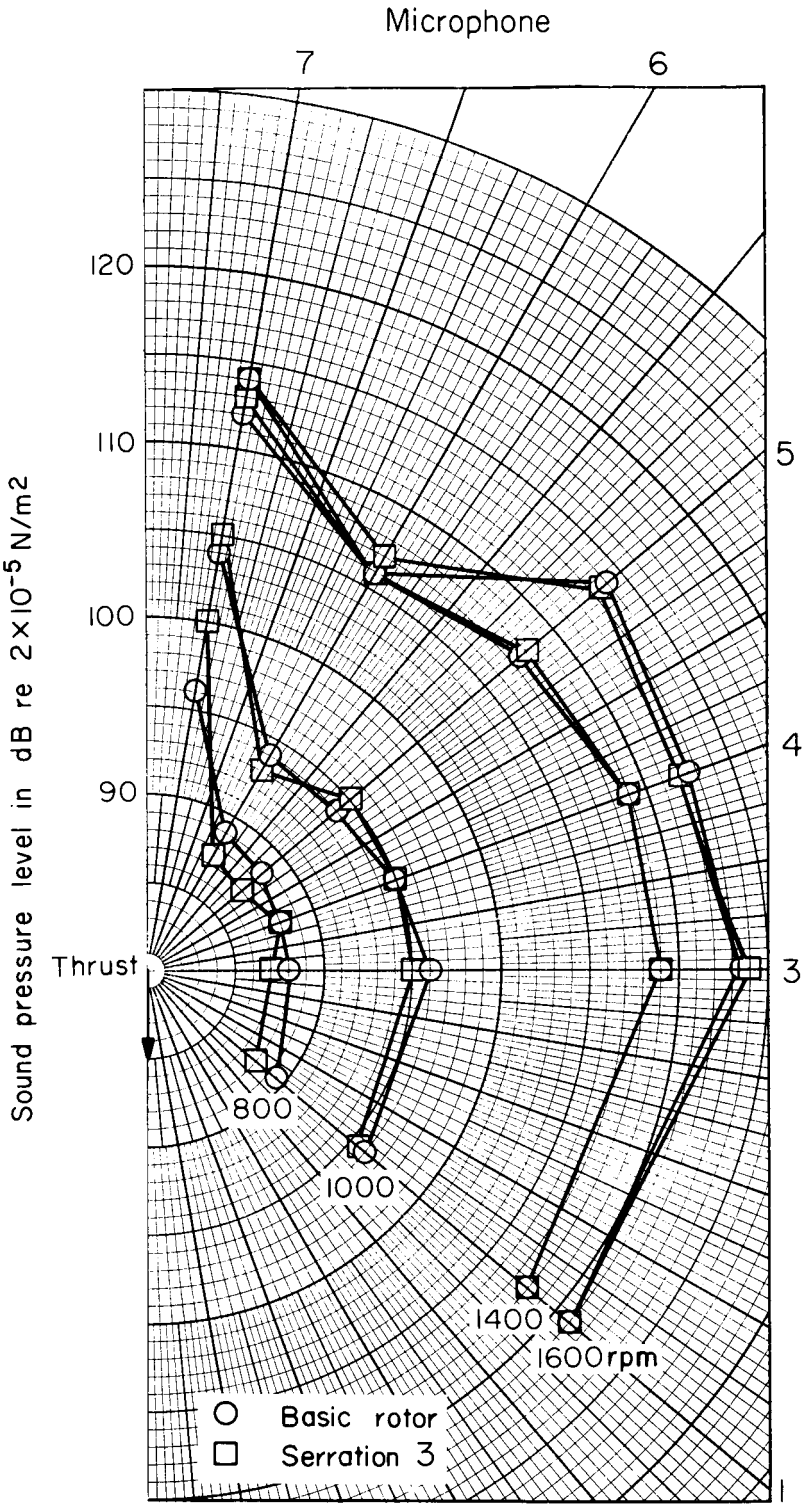

(e) Position 2, $\beta = 12°$.

Figure 10.– Continued.

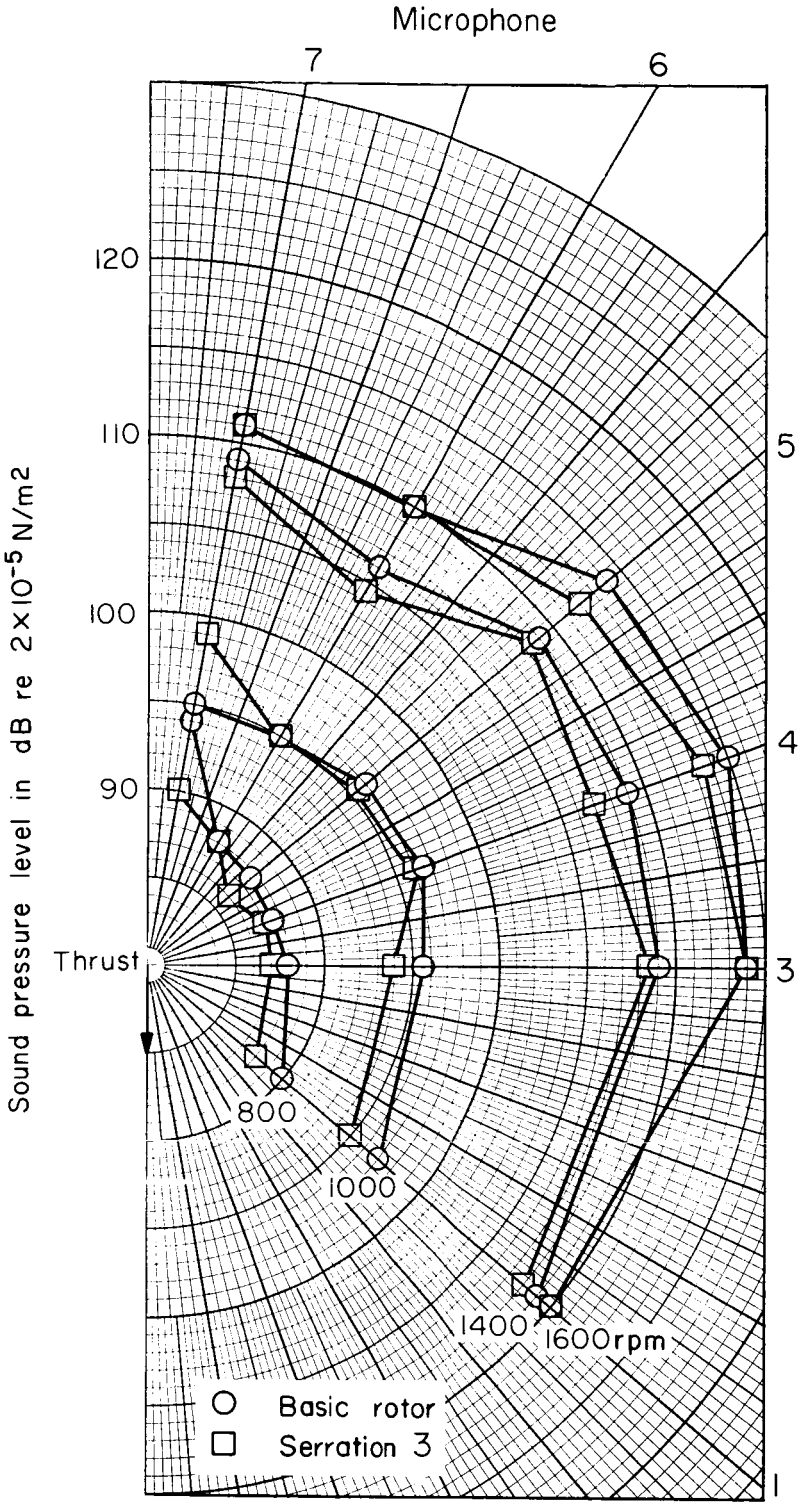

(f) Position 3, $\beta = 12°$.

Figure 10.– Continued.

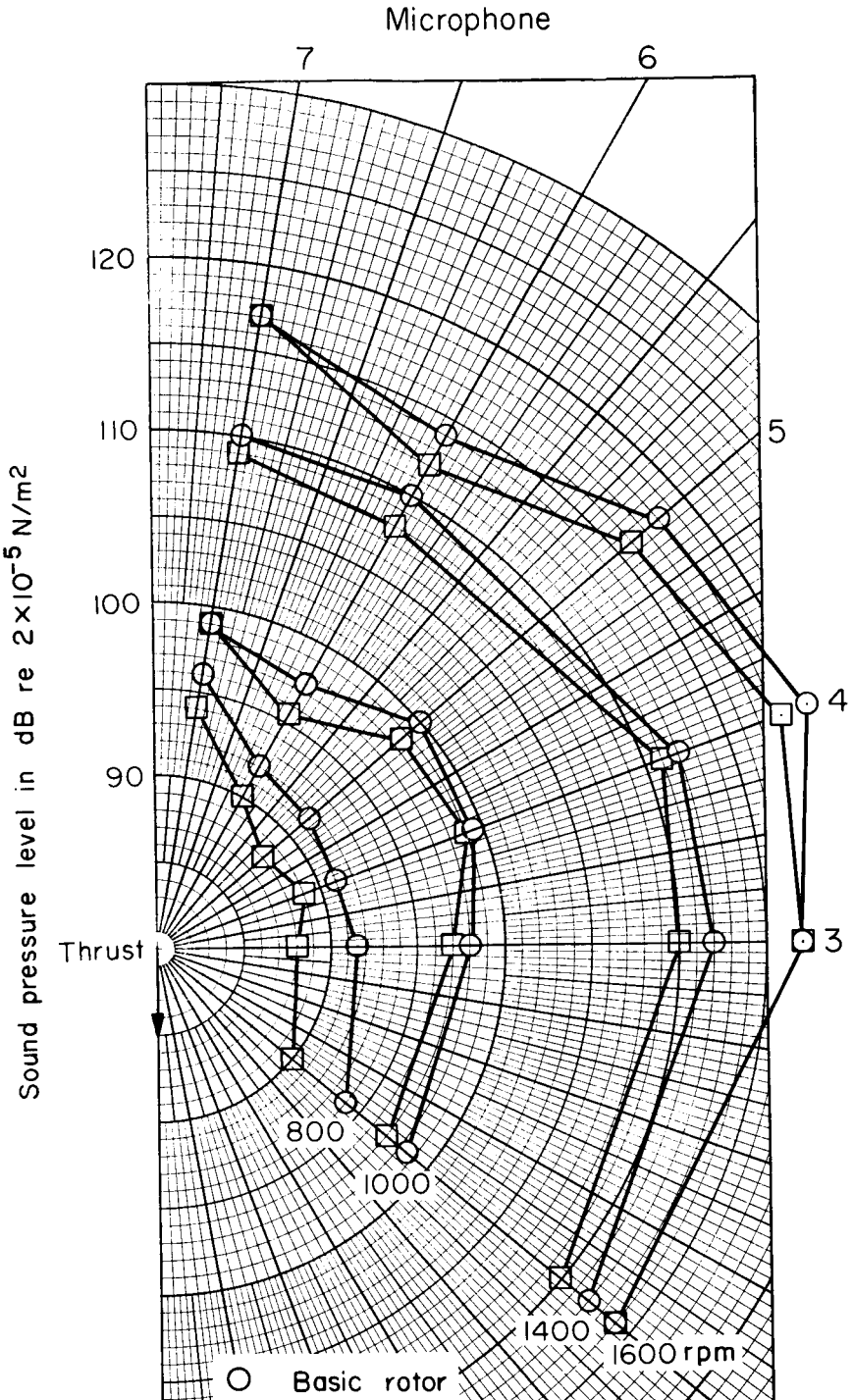

(g) Position 3, $\beta = 18°$.

Figure 10.– Concluded.

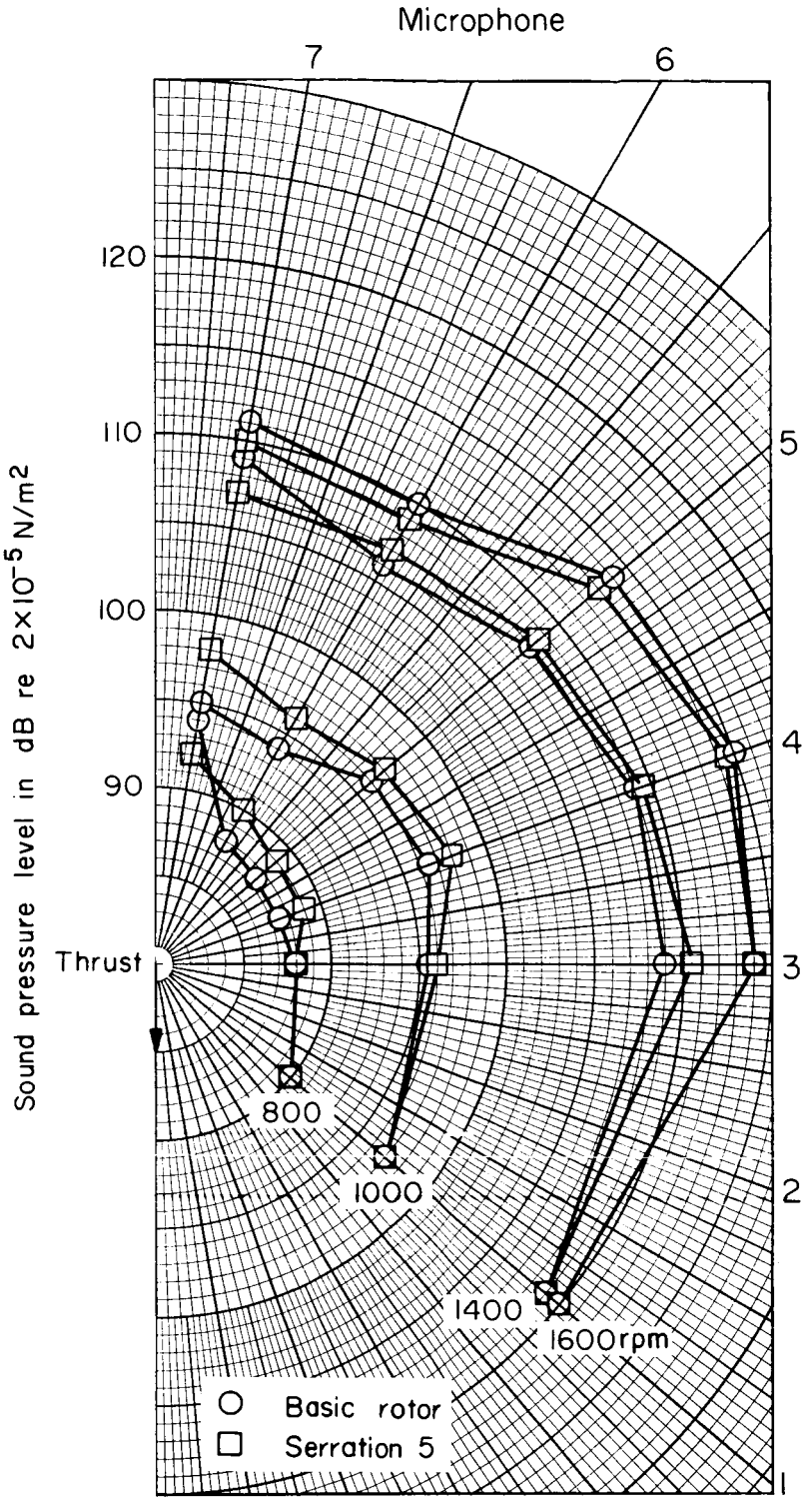

(a) Position 1, $\beta = 12°$.

Figure 11.– Overall sound pressure levels at 7.6 m (25 ft) from the large-scale rotor with and without serration 5.

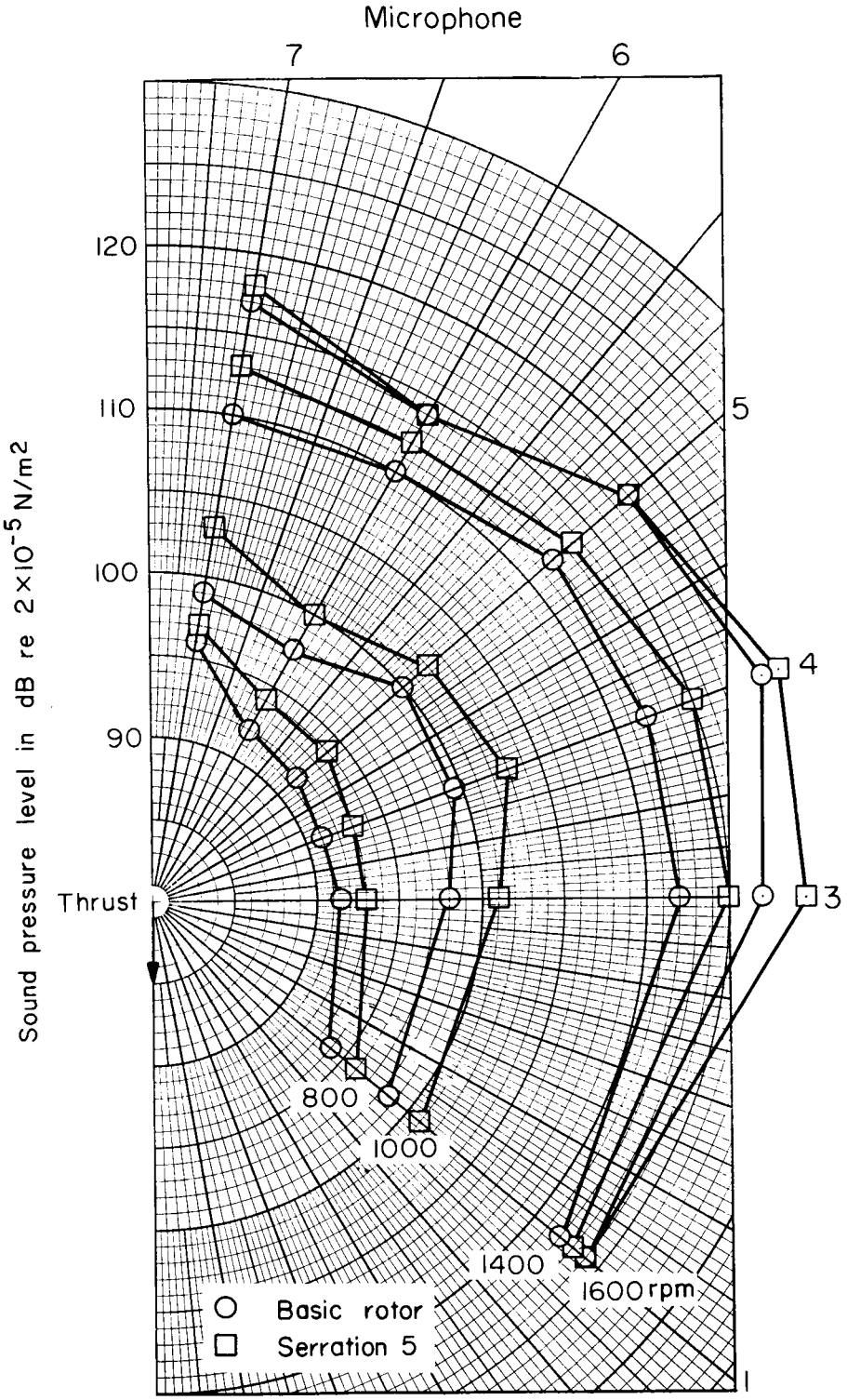

(b) Position 1, $\beta = 18°$.

Figure 11.– Continued.

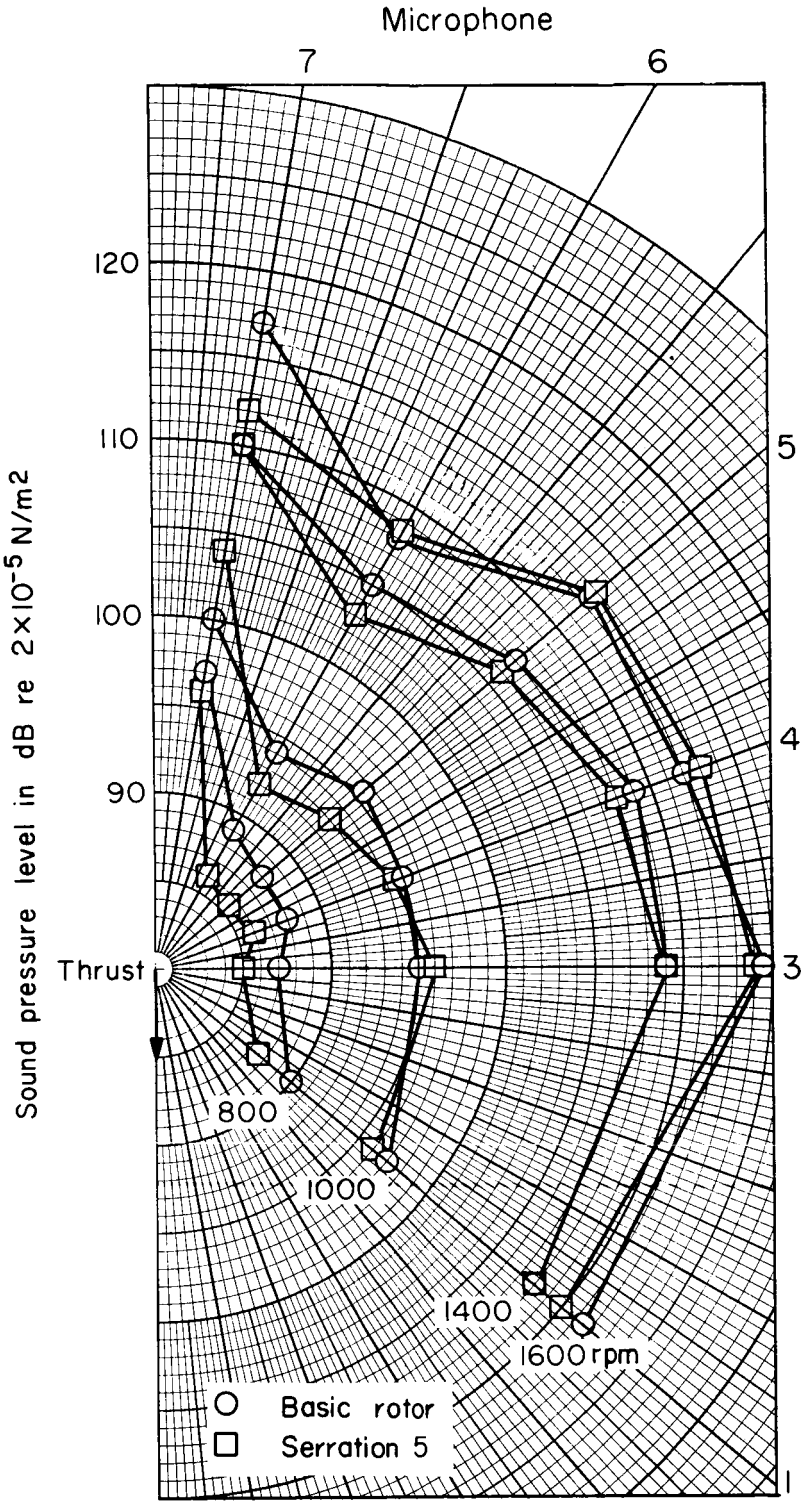

(c) Position 2, $\beta = 12°$.

Figure 11.– Continued.

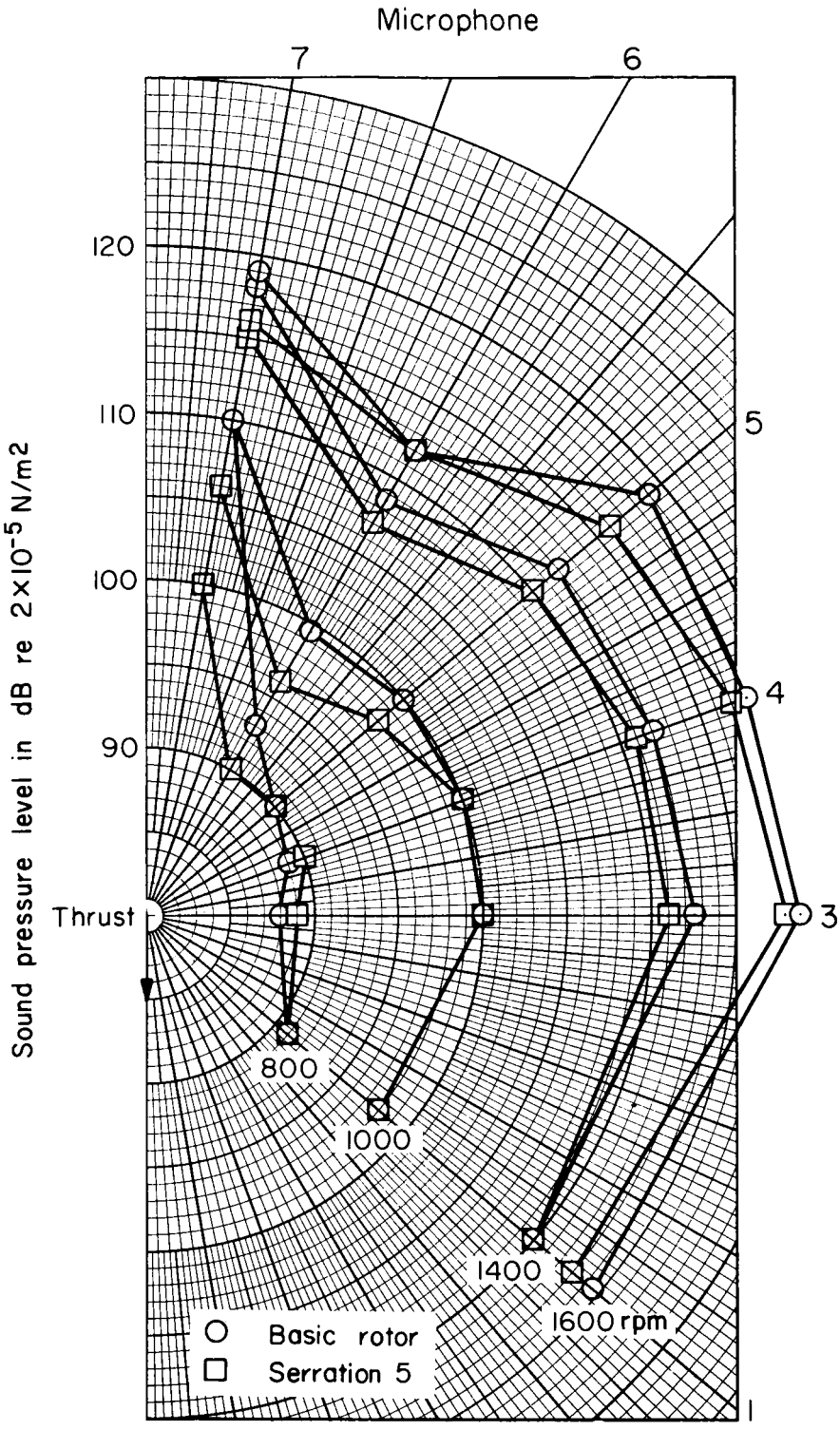

(d) Position 2, $\beta = 18°$.

Figure 11.– Continued.

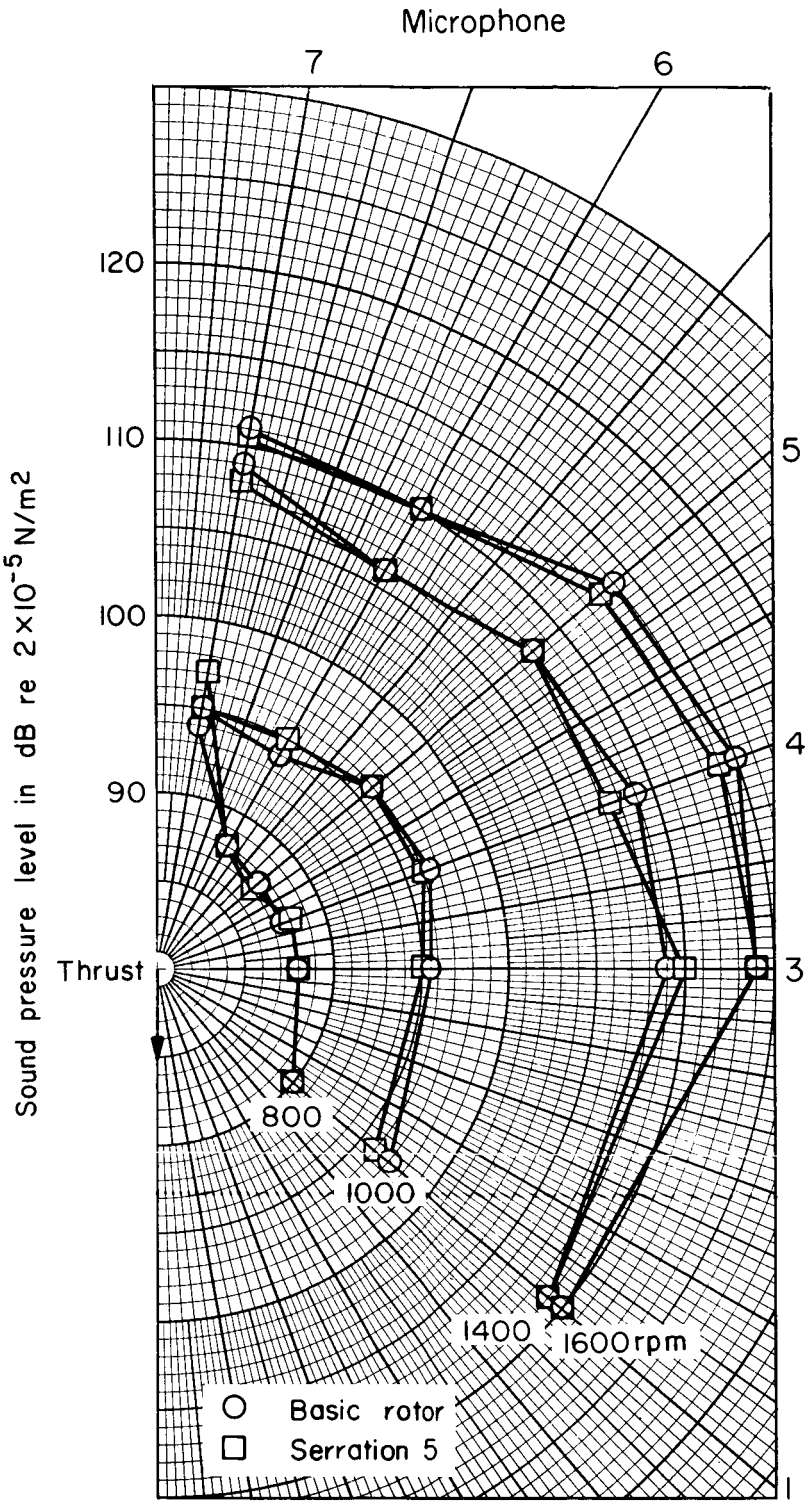

(e) Position 3, $\beta = 12°$.

Figure 11.– Continued.

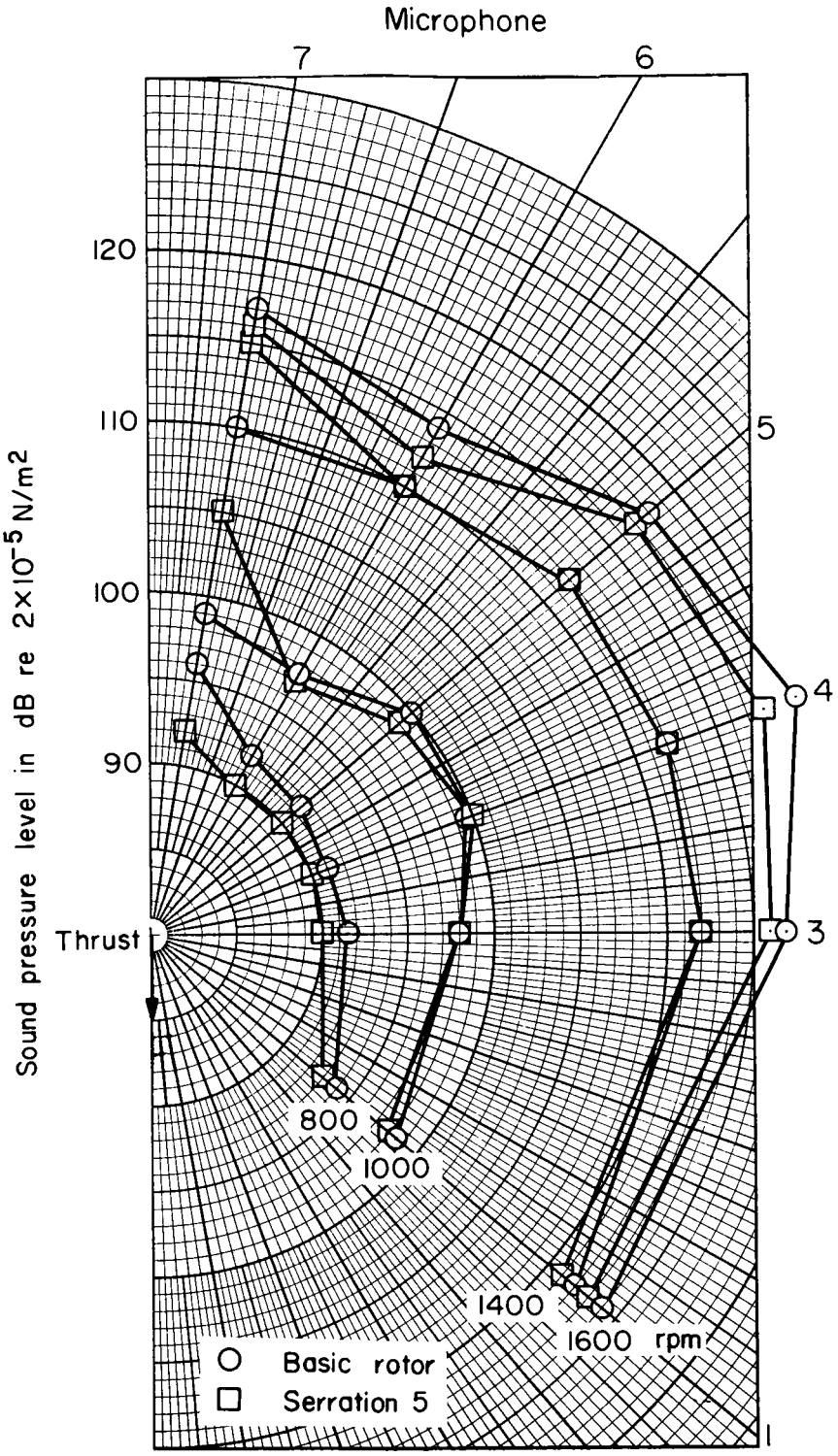

(f) Position 3, $\beta = 18°$.

Figure 11.– Concluded.

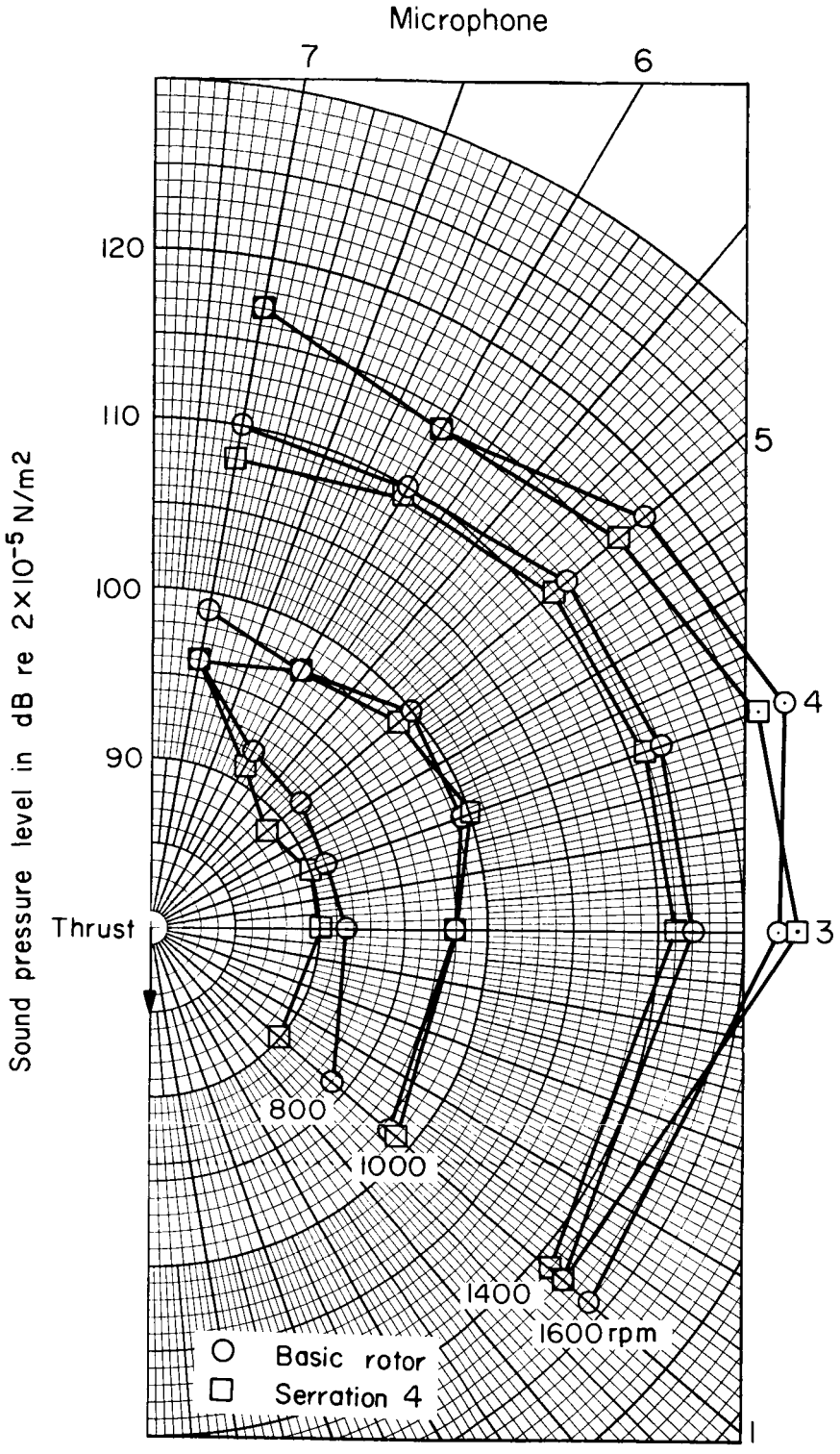

(a) Position 1, $\beta = 18°$.

Figure 12.– Overall sound pressure levels at 7.6 m (25 ft) from the large-scale rotor, with and without serration 4.

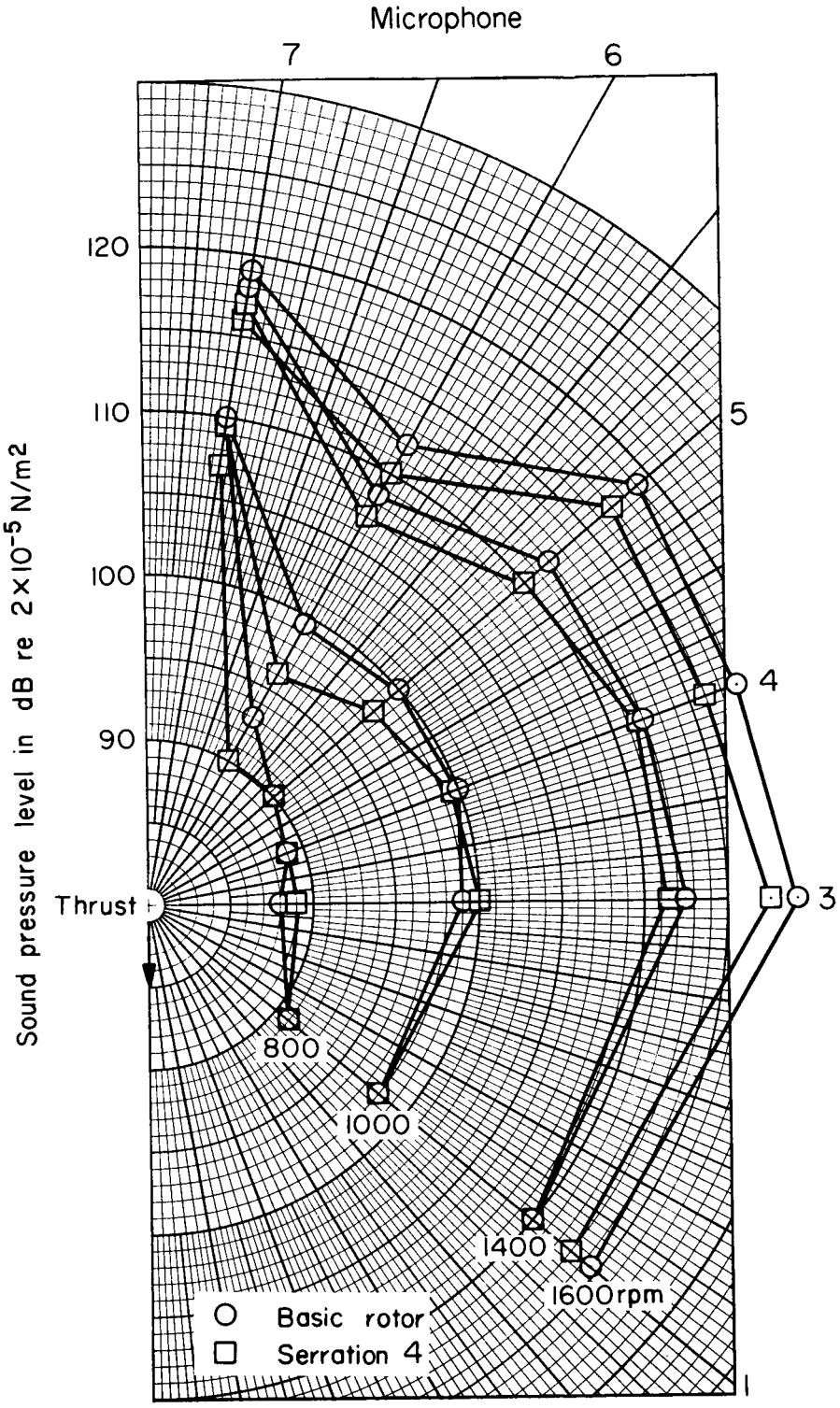

(b) Position 2, $\beta = 18°$.

Figure 12.– Continued.

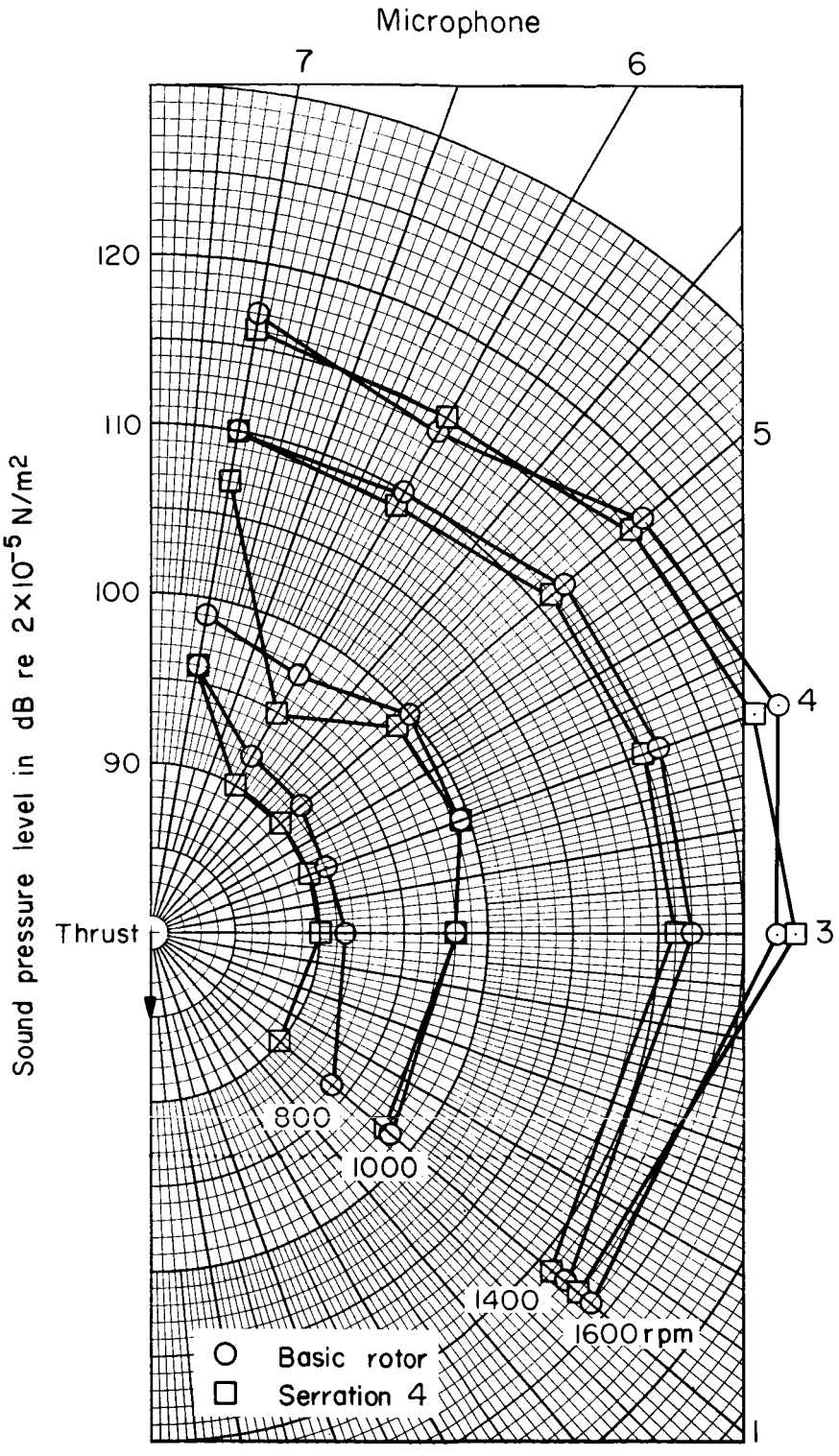

(c) Position 3, $\beta = 18°$.

Figure 12.– Concluded.

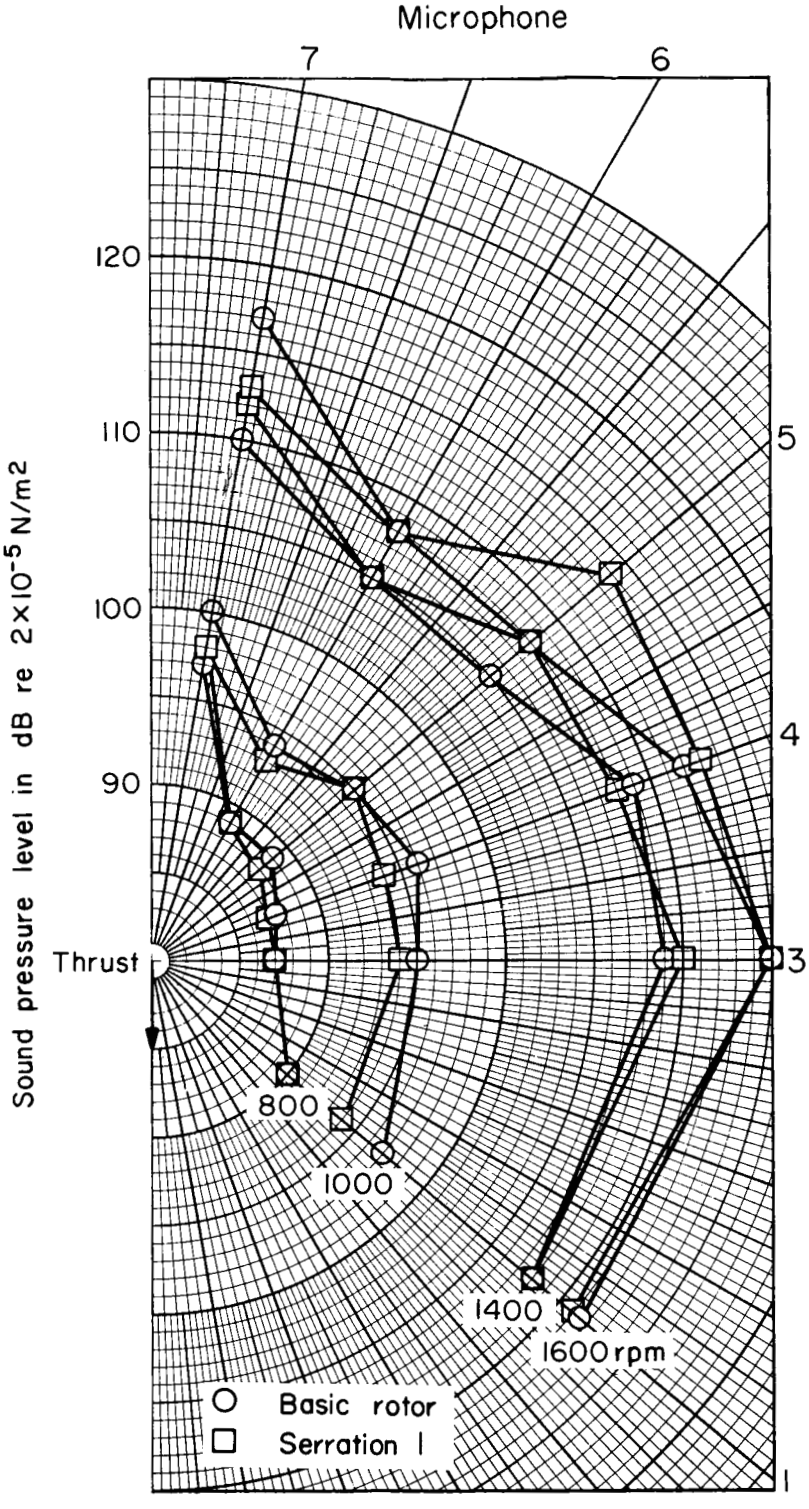

Figure 13.– Overall sound pressure levels at 7.6 m (25 ft) from the large-scale rotor, with and without serration 1 at position 2; $\beta = 12°$.

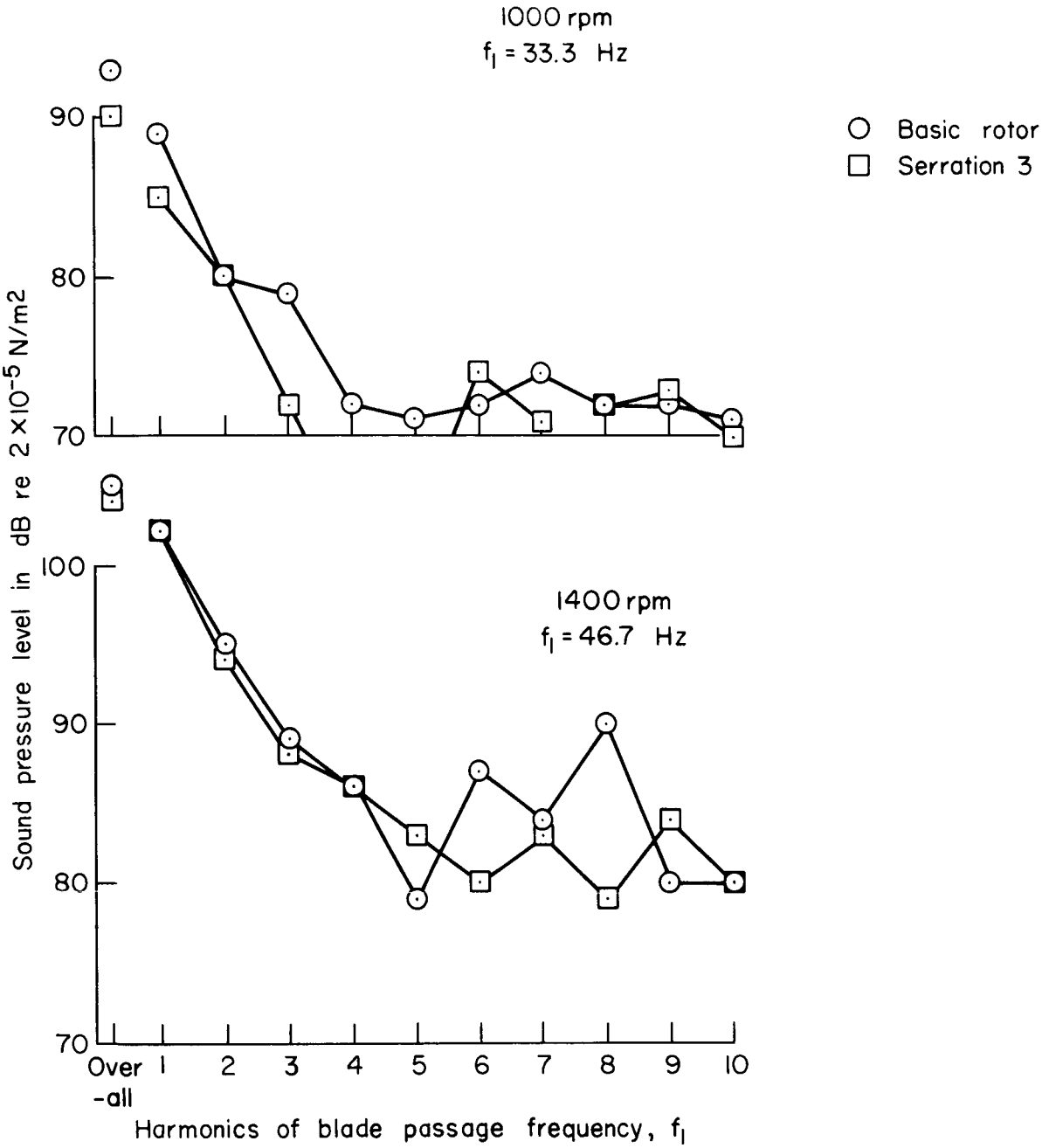

(a) Position 2, $\beta = 6°$.

Figure 14.– Sound pressure levels at harmonics of blade passage frequency of the large-scale rotor, with and without serration 3; measured at microphone 5.

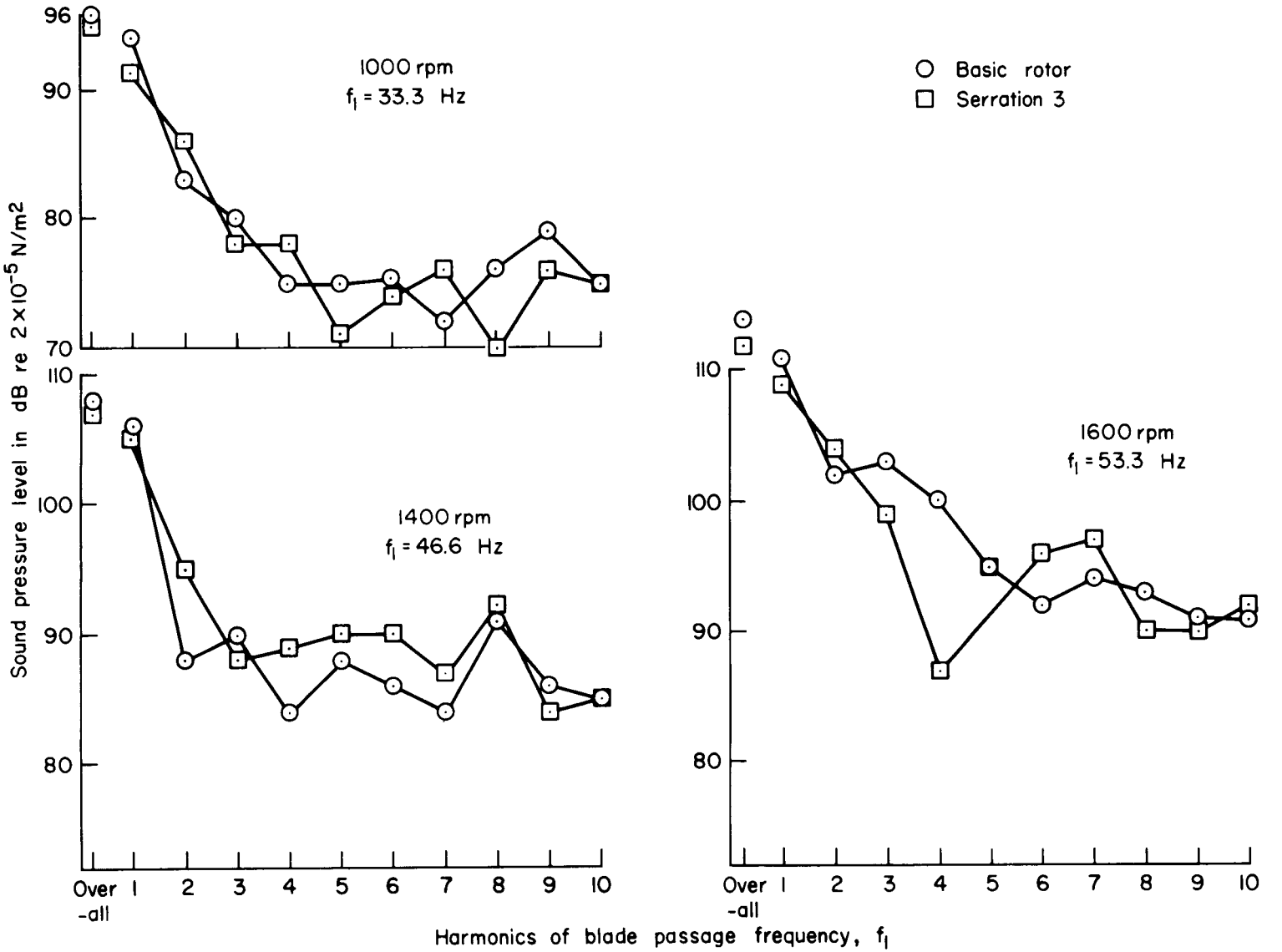

(b) Position 3, $\beta = 12°$.

Figure 14.– Continued.

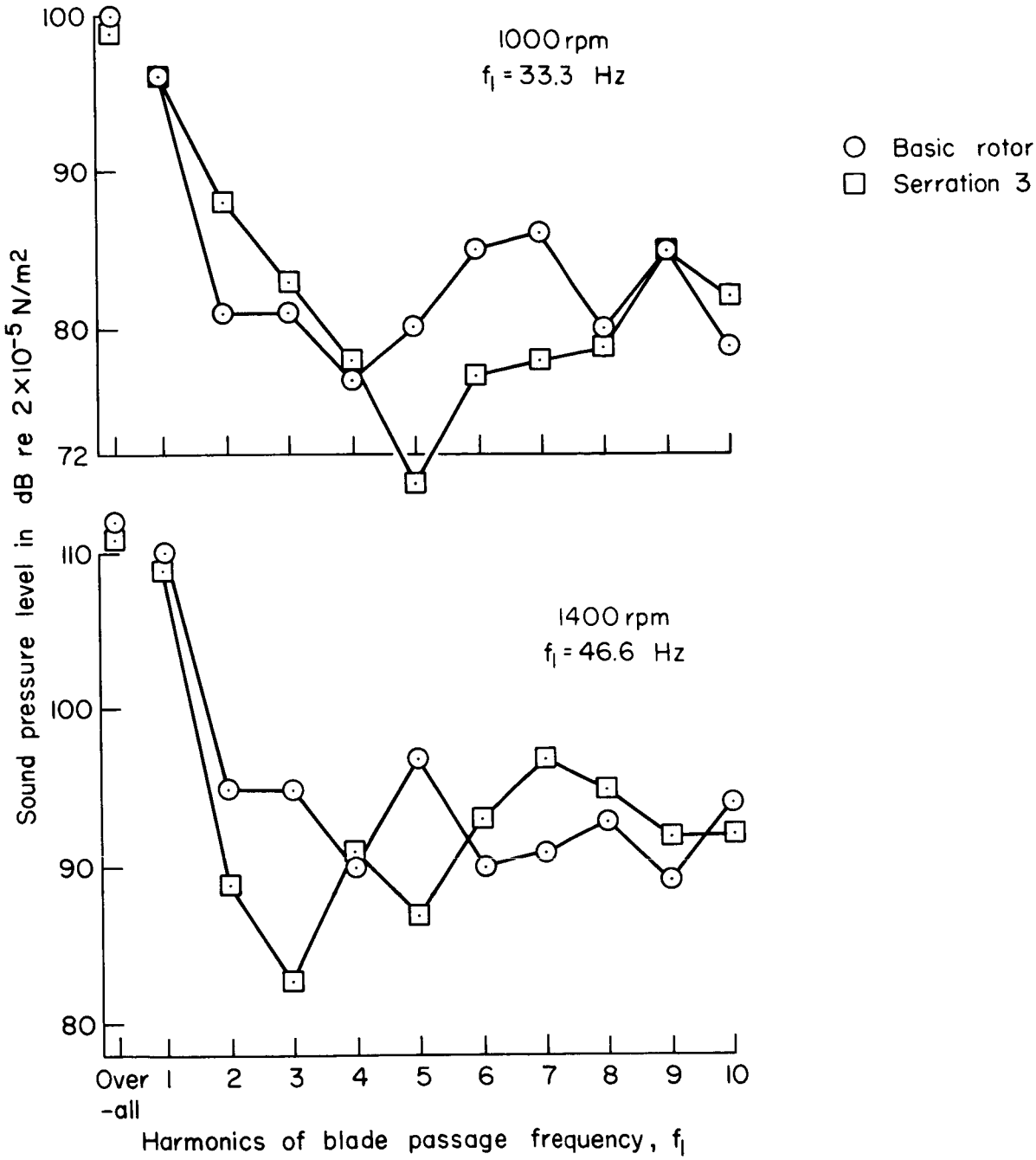

(c) Position 3, $\beta = 18°$.

Figure 14.– Concluded.

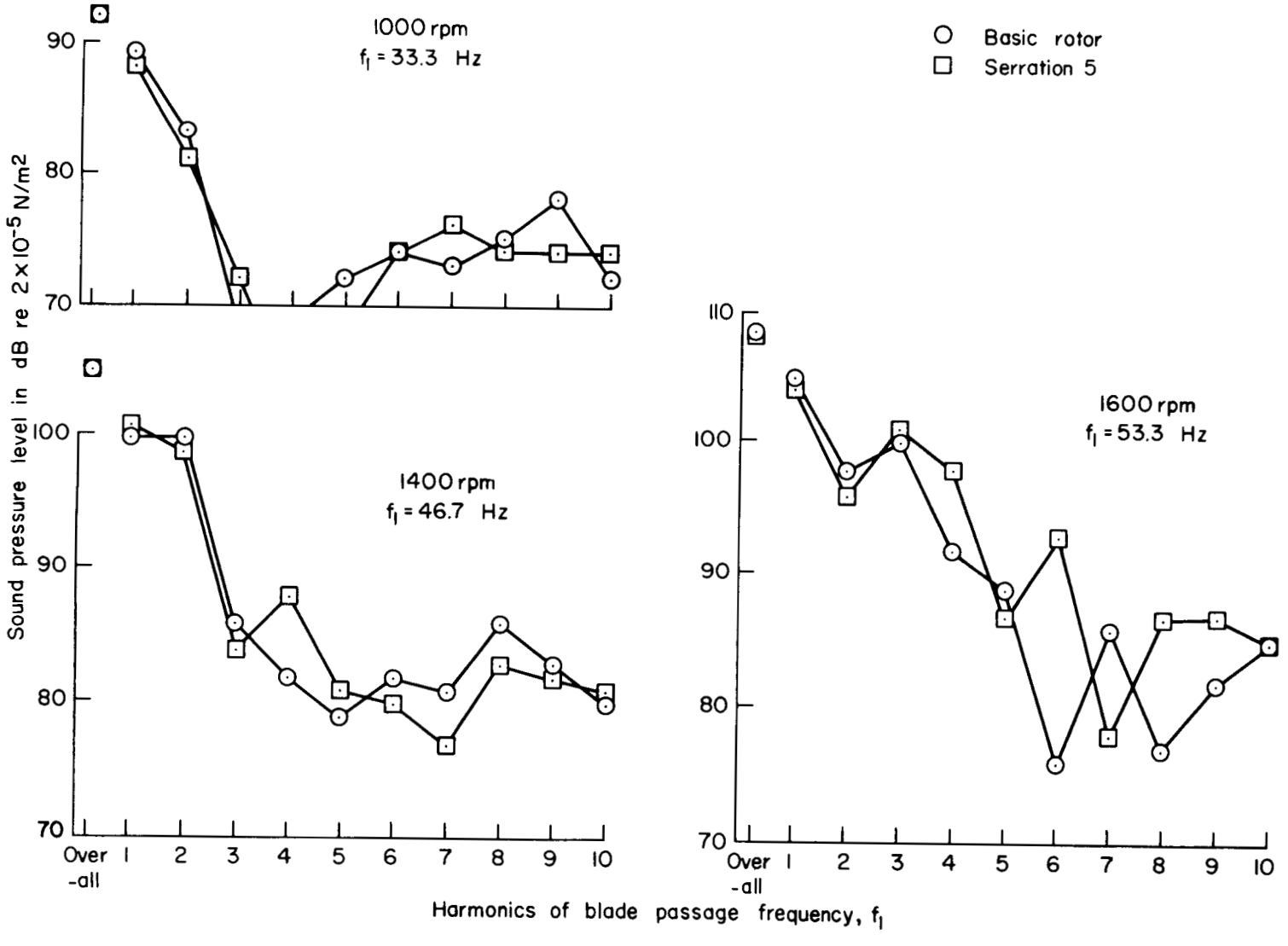

(a) Position 3, $\beta = 6°$.

Figure 15.– Sound pressure levels at harmonics of blade passage frequency of the large-scale rotor, with and without serration 5; measured at microphone 5.

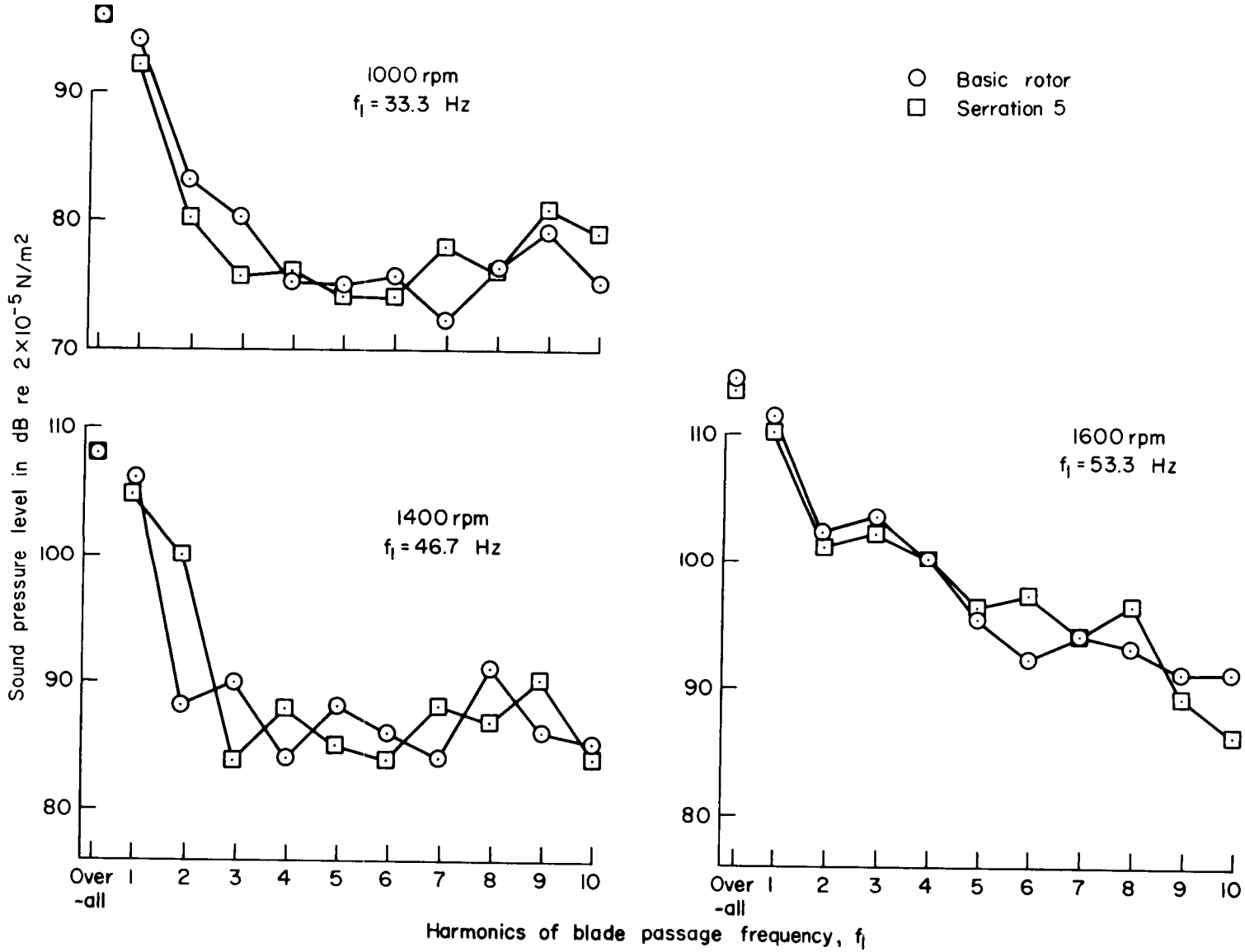

(b) Position 3, $\beta = 12°$.

Figure 15.– Continued.

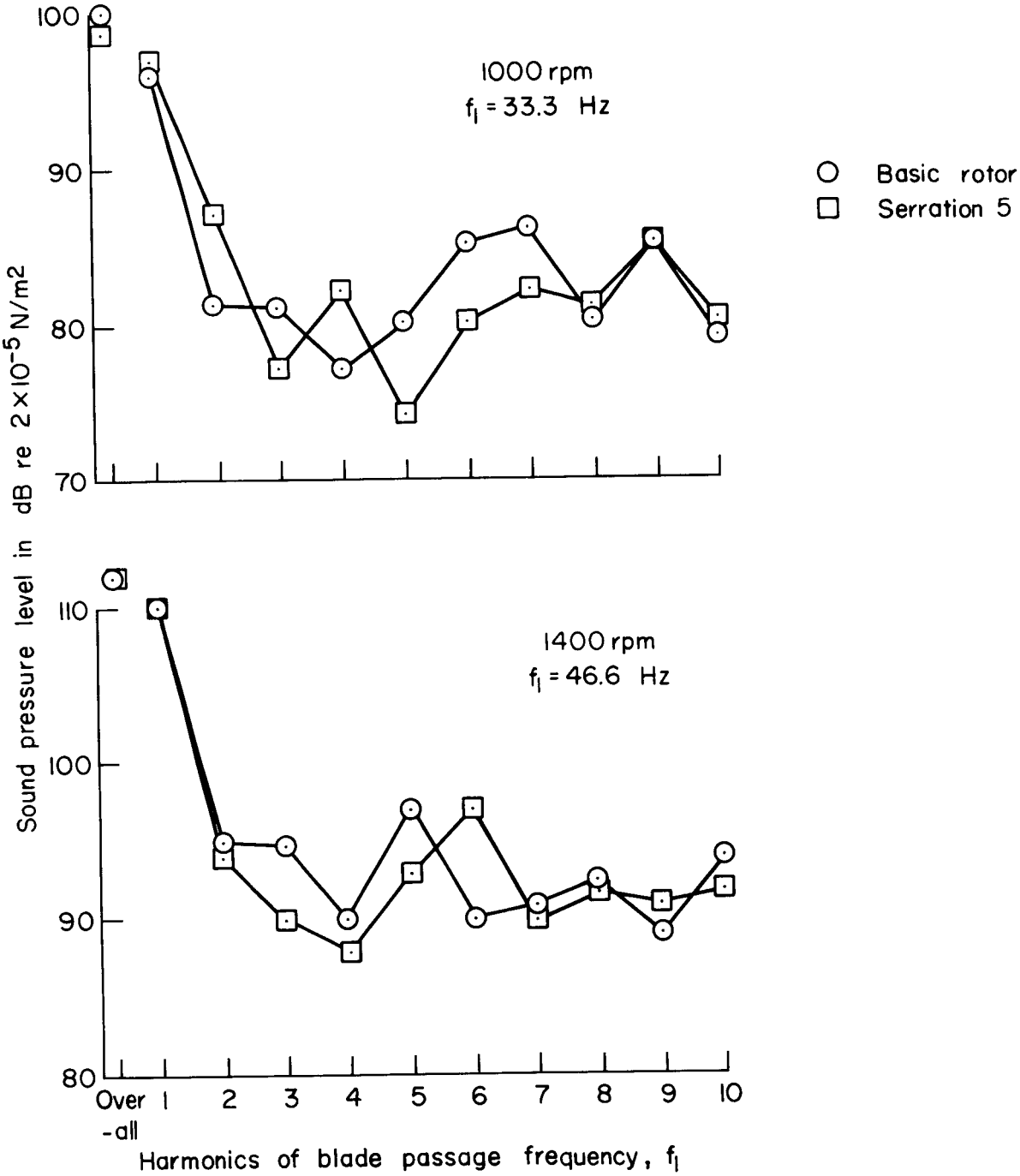

(c) Position 3, $\beta = 18°$.

Figure 15.– Concluded.

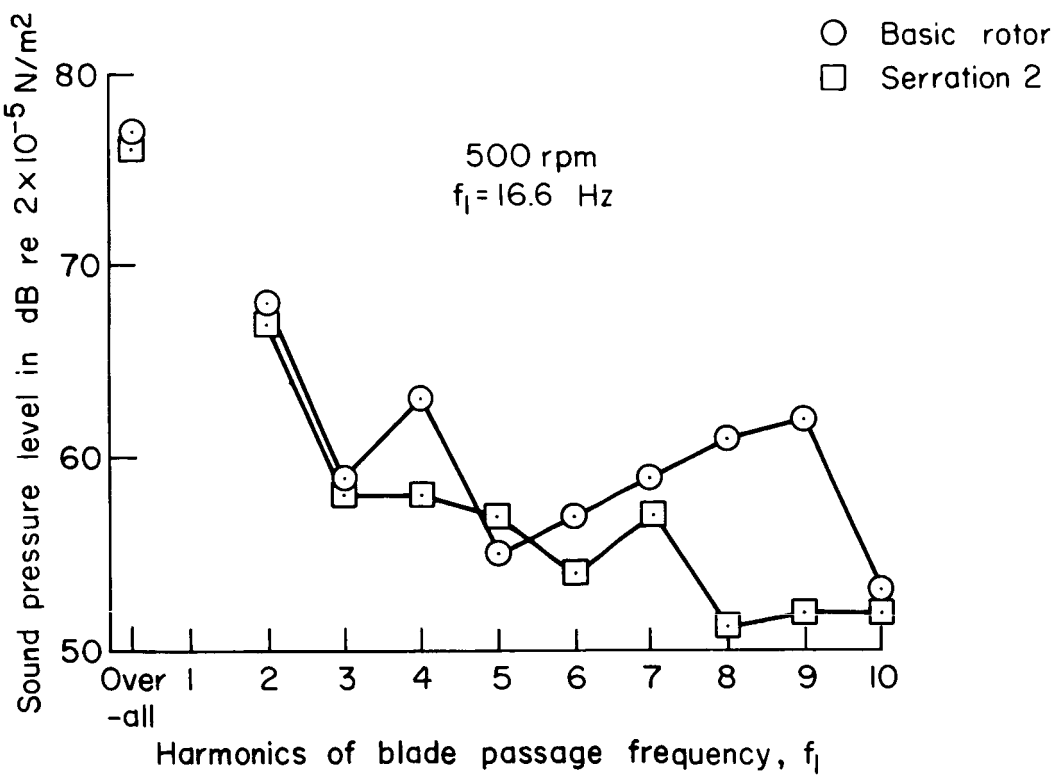

Figure 16.– Sound pressure levels at harmonics of blade passage frequency of the large-scale rotor, with and without serration 2 at position 3, $\beta = 6°$; measured at microphone 5.

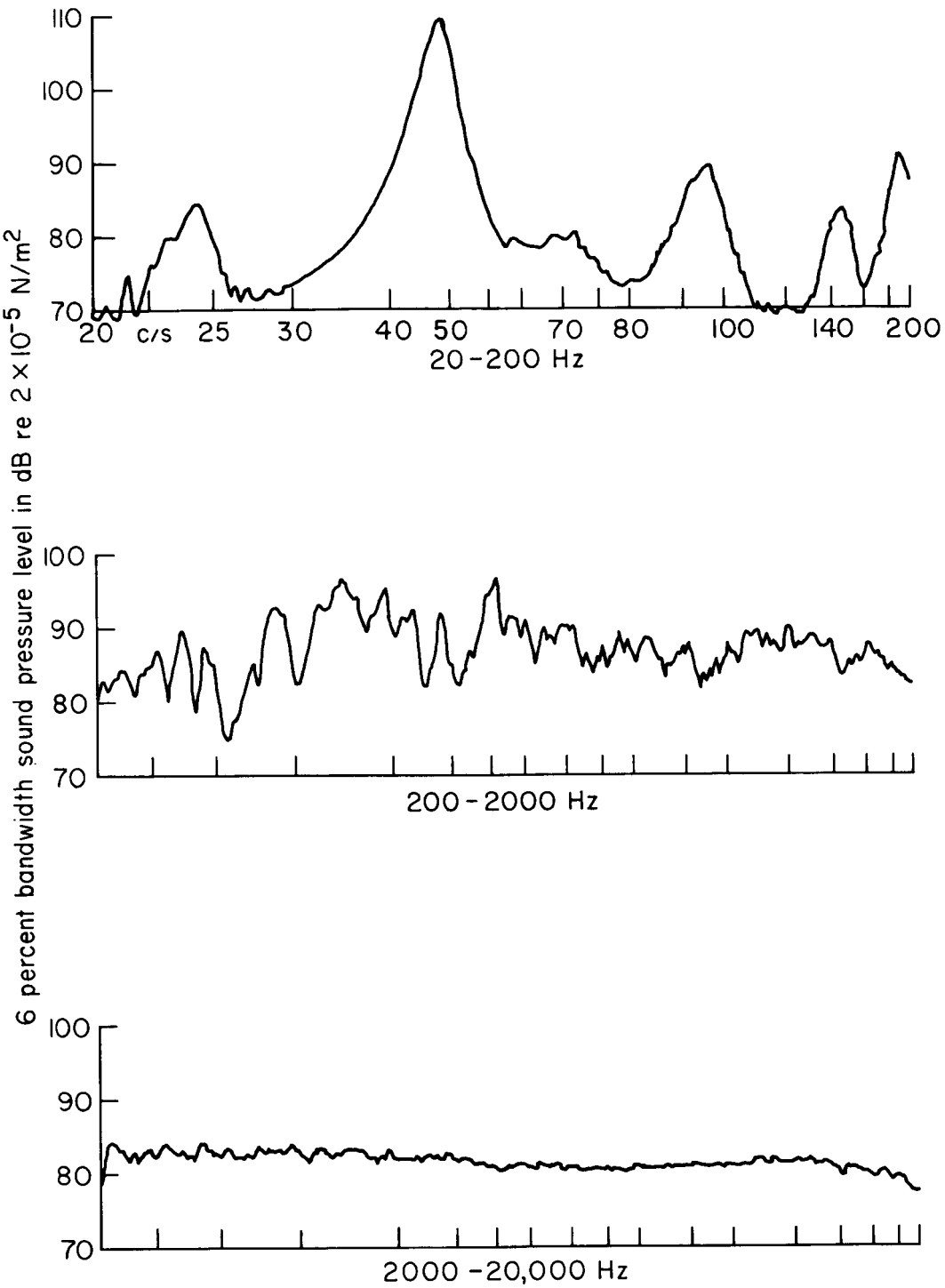

(a) Serration 3, position 3.

Figure 17.– Narrow band spectrum sound pressure level at microphone 5; $\beta = 18°$, 1400 rpm.

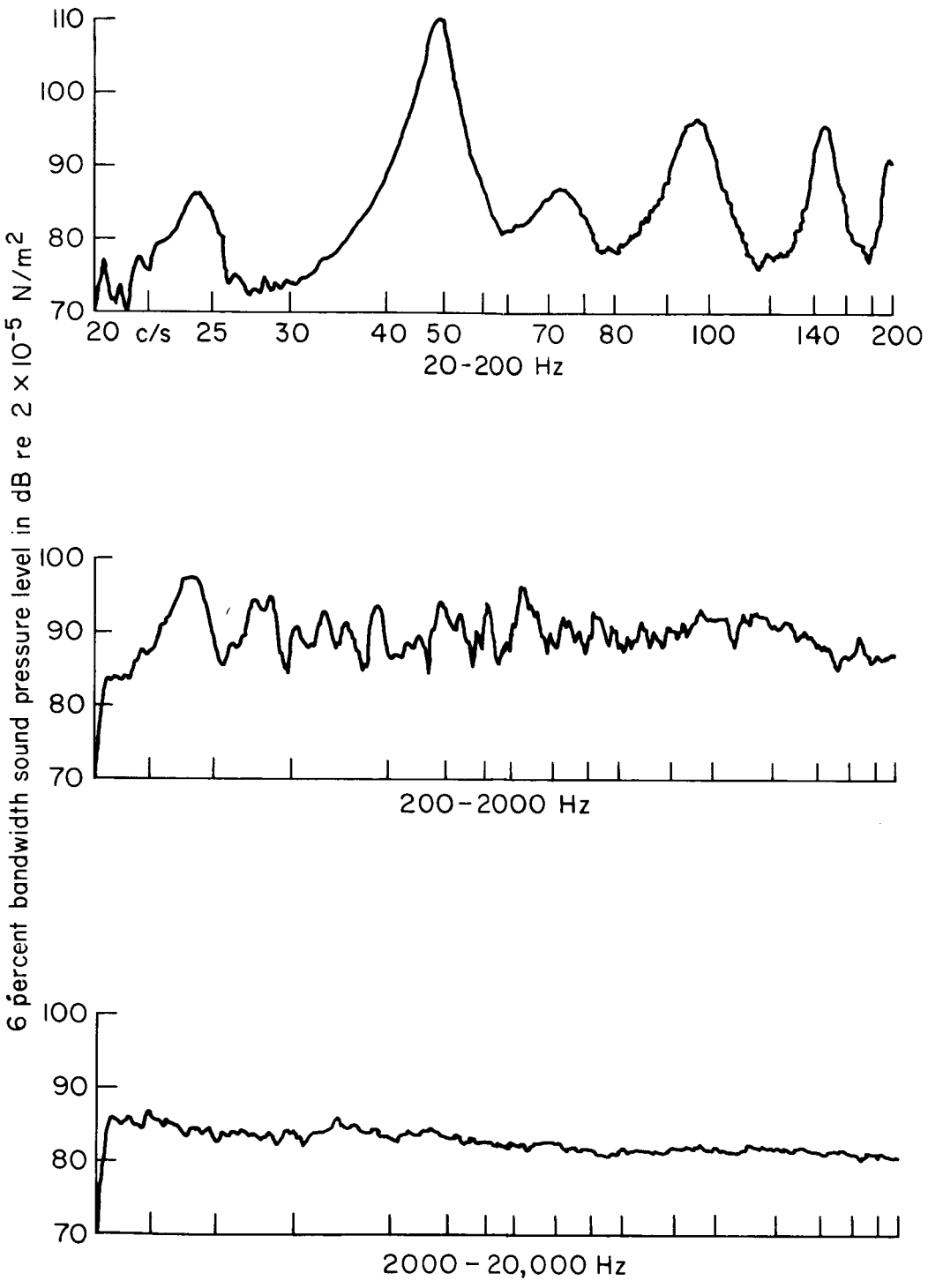

(b) Basic rotor.

Figure 17.– Concluded.

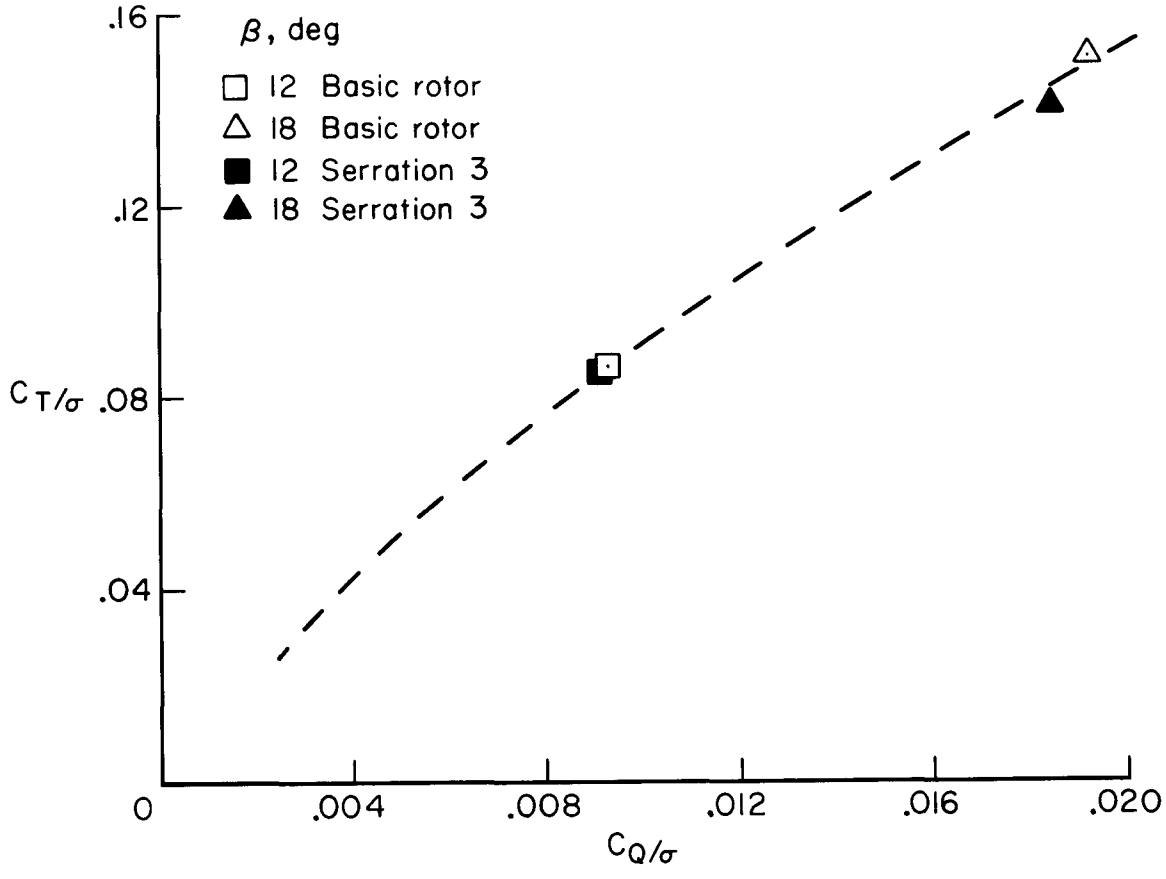

(a) 800 rpm, position 3.

Figure 18.– Thrust parameter C_T/σ versus torque parameter C_Q/σ for the large-scale rotor, with and without serration 3.

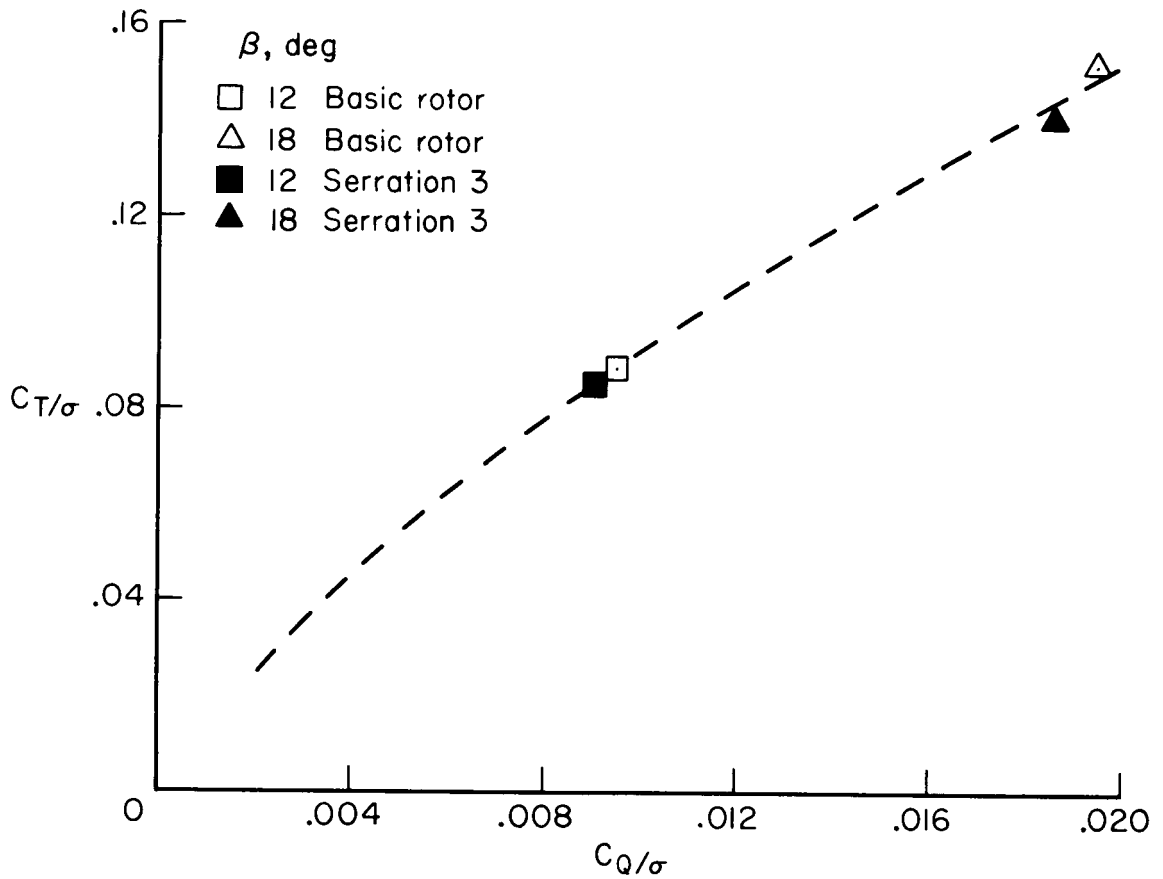

(b) 1000 rpm, position 3.

Figure 18.– Continued.

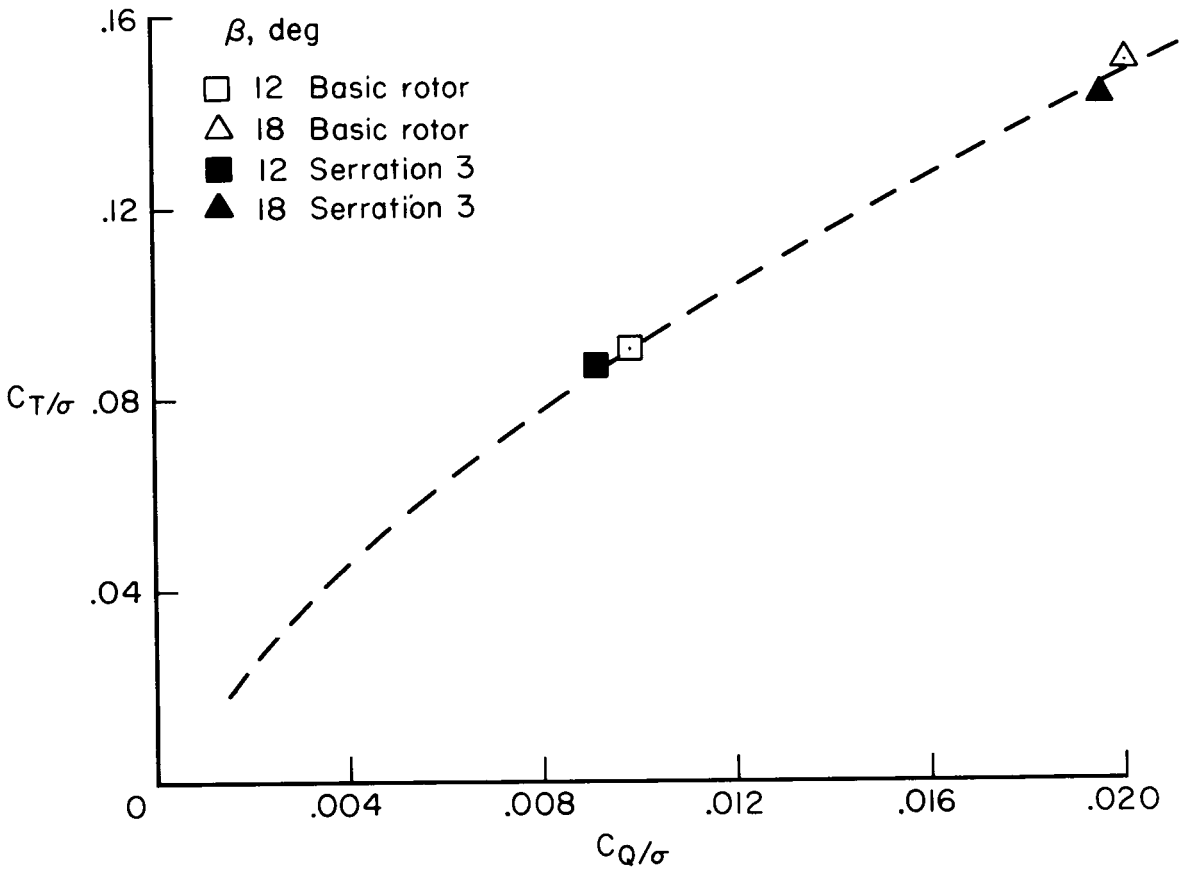

(c) 1400 rpm, position 3.

Figure 18.– Continued.

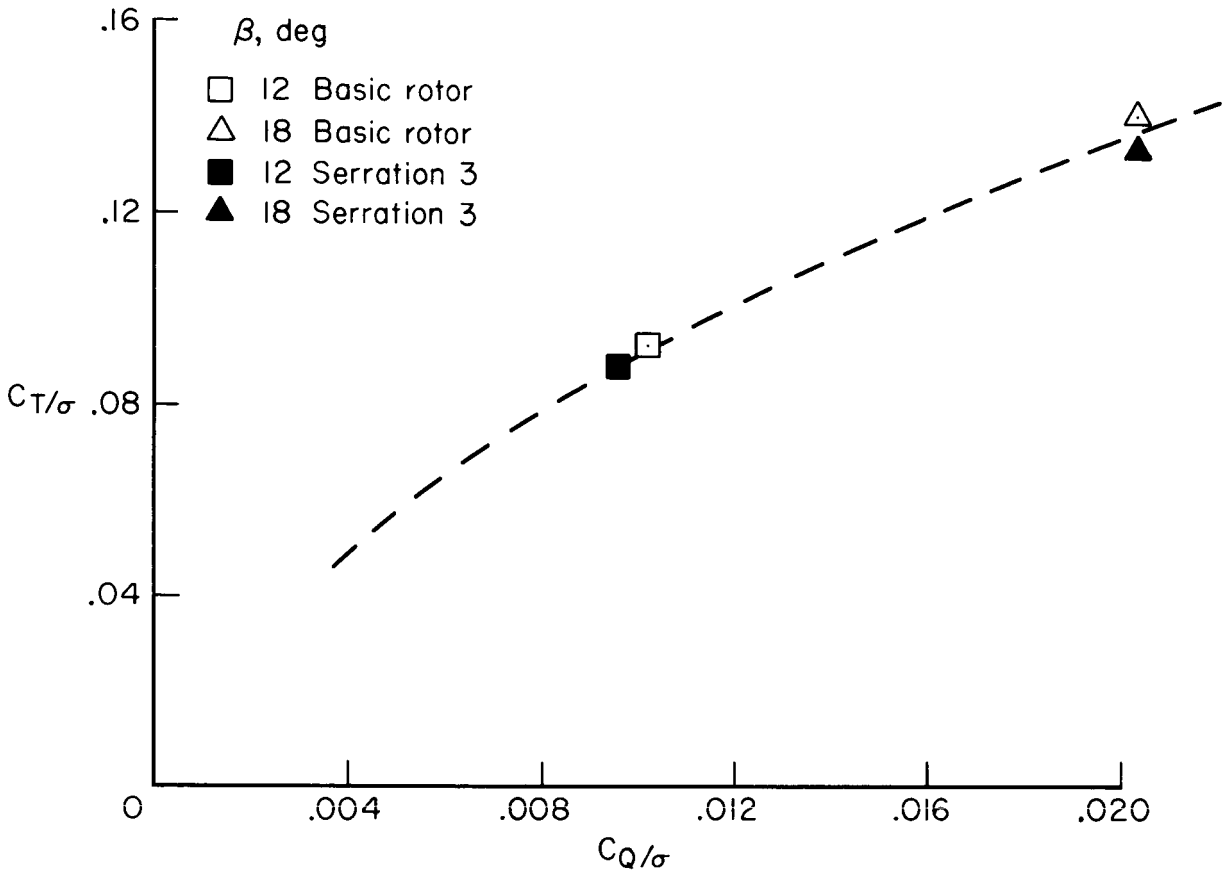

(d) 1600 rpm, position 3.

Figure 18.– Continued.

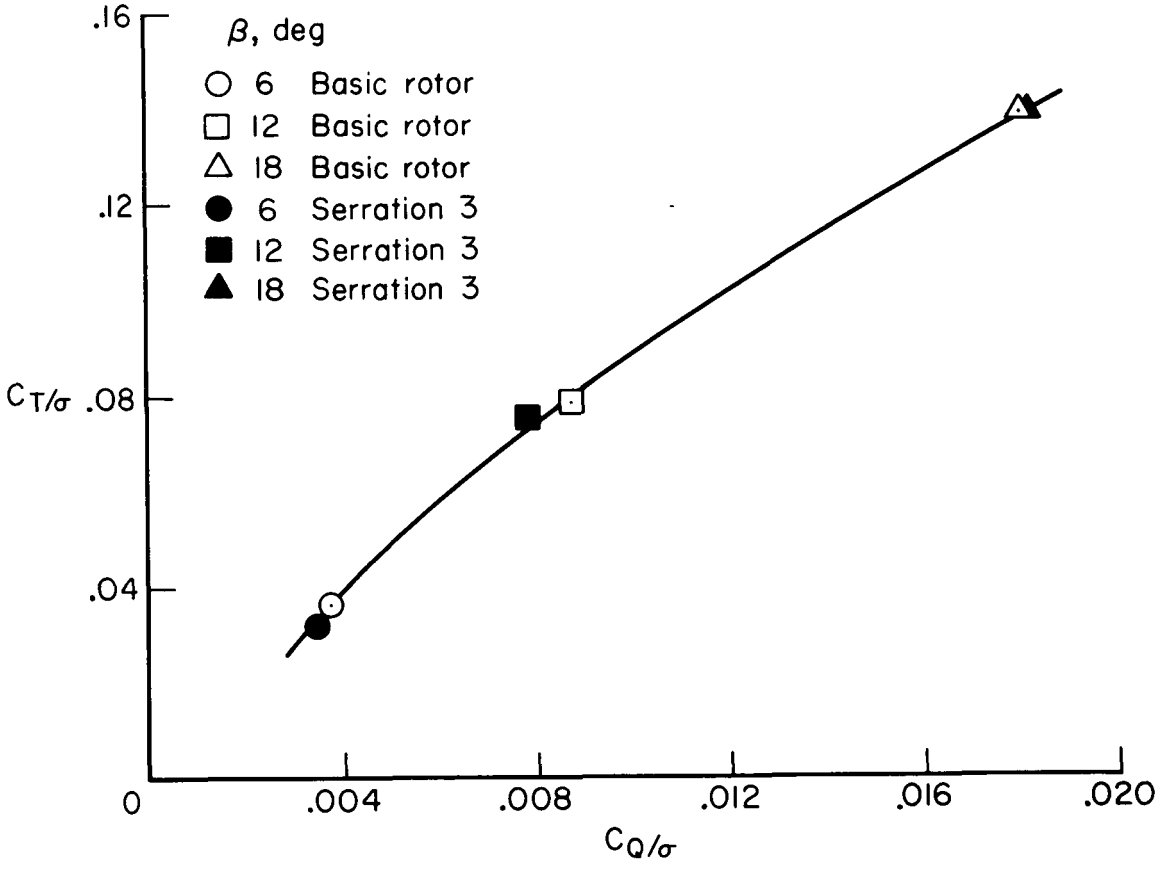

(e) 800 rpm, position 1.

Figure 18.– Continued.

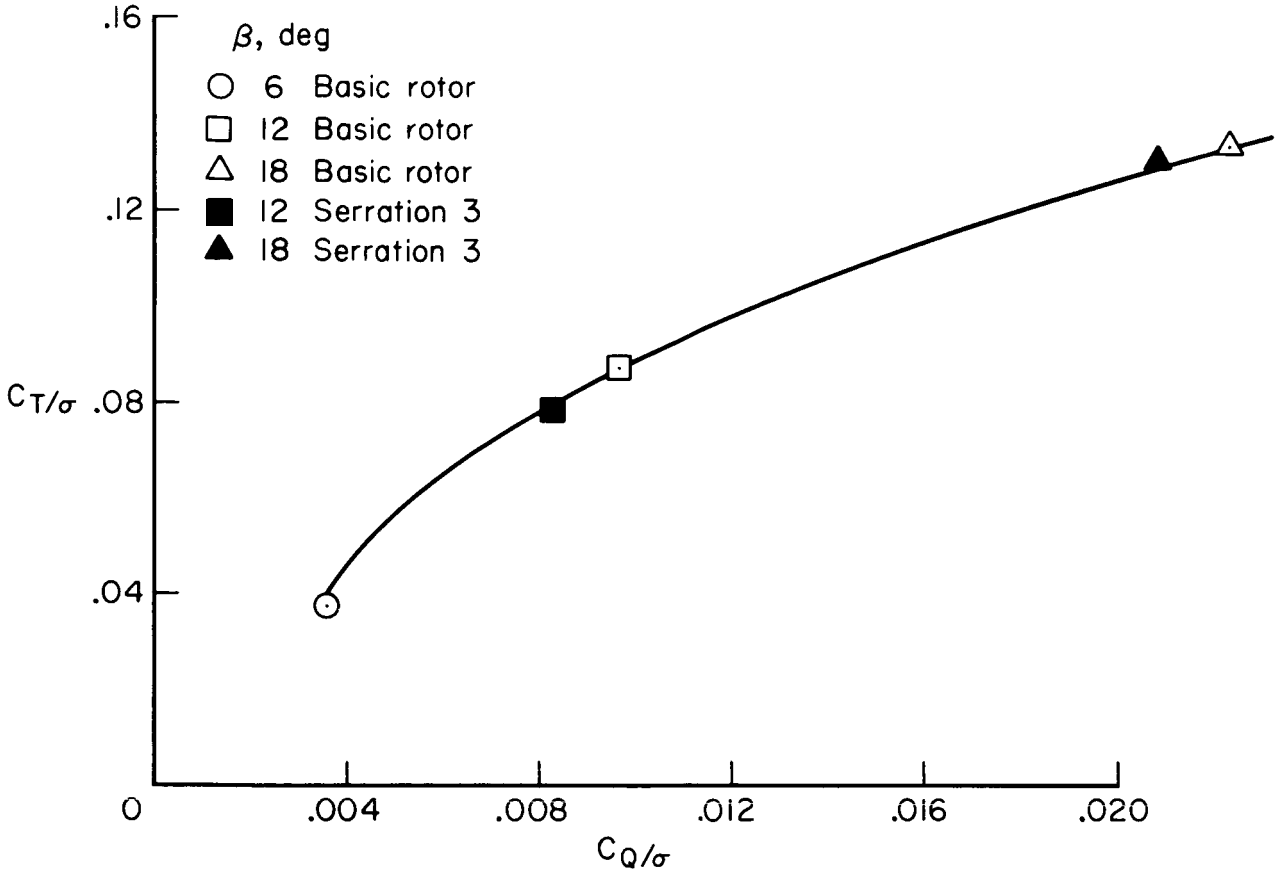

(f) 1600 rpm, position 1.

Figure 18.– Concluded.

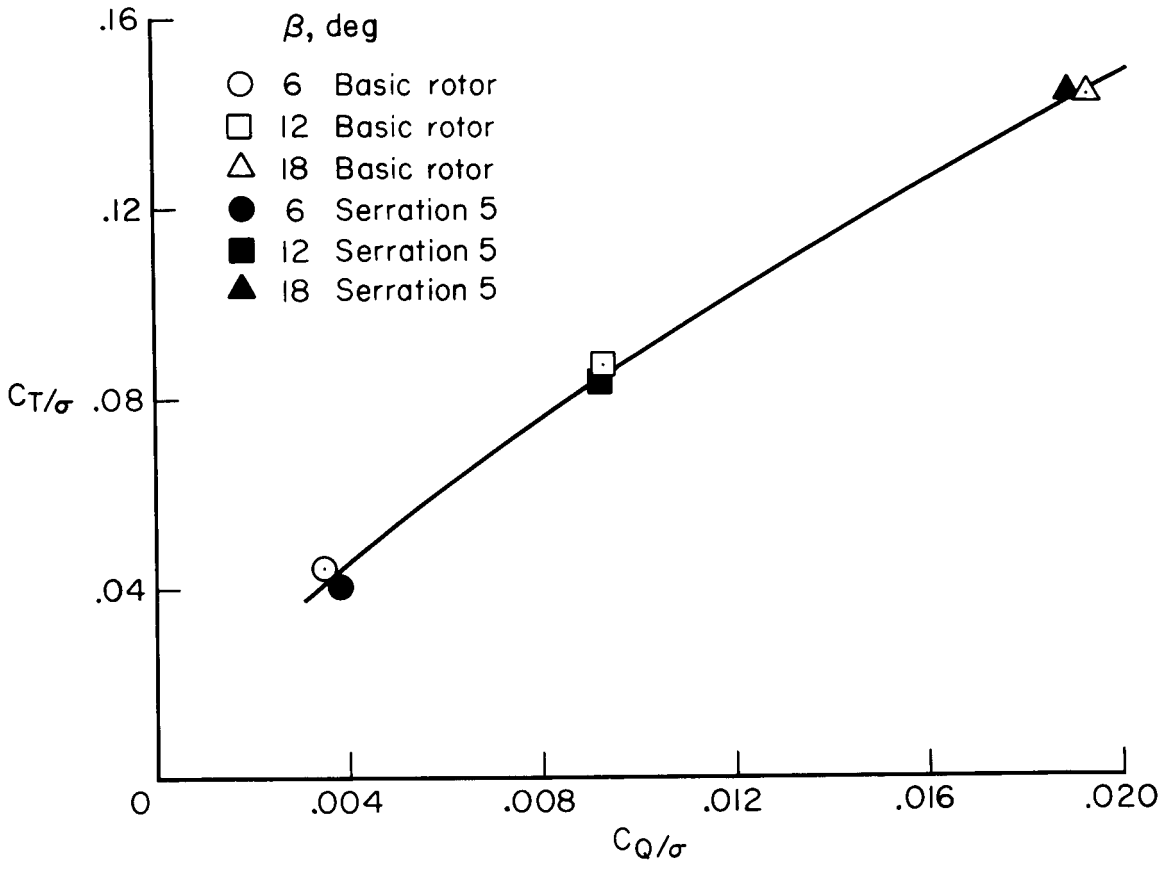

(a) 800 rpm, position 3.

Figure 19.– Thrust parameter C_T/σ versus torque parameter C_Q/σ for the large-scale rotor, with and without serration 5.

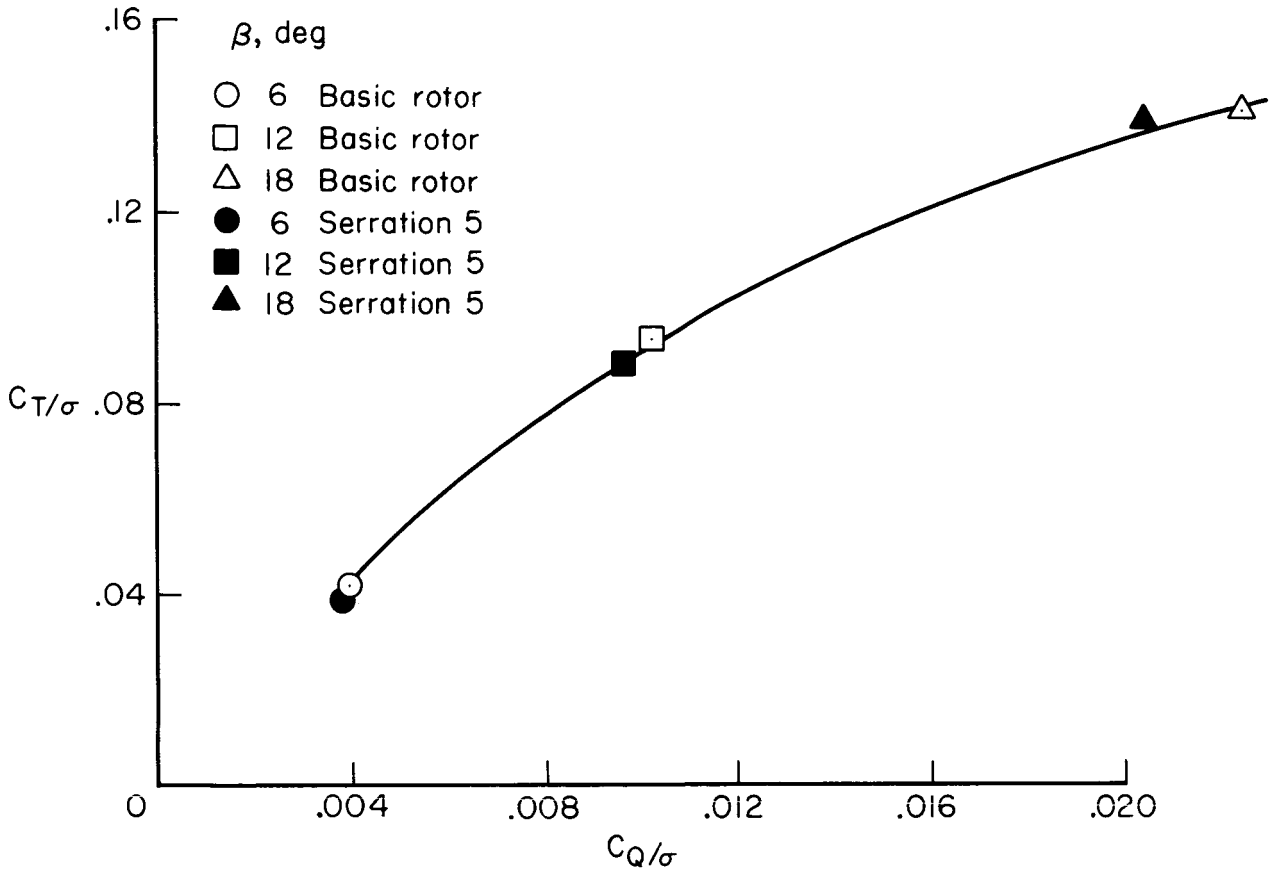

(b) 1600 rpm, position 3.

Figure 19.– Concluded.

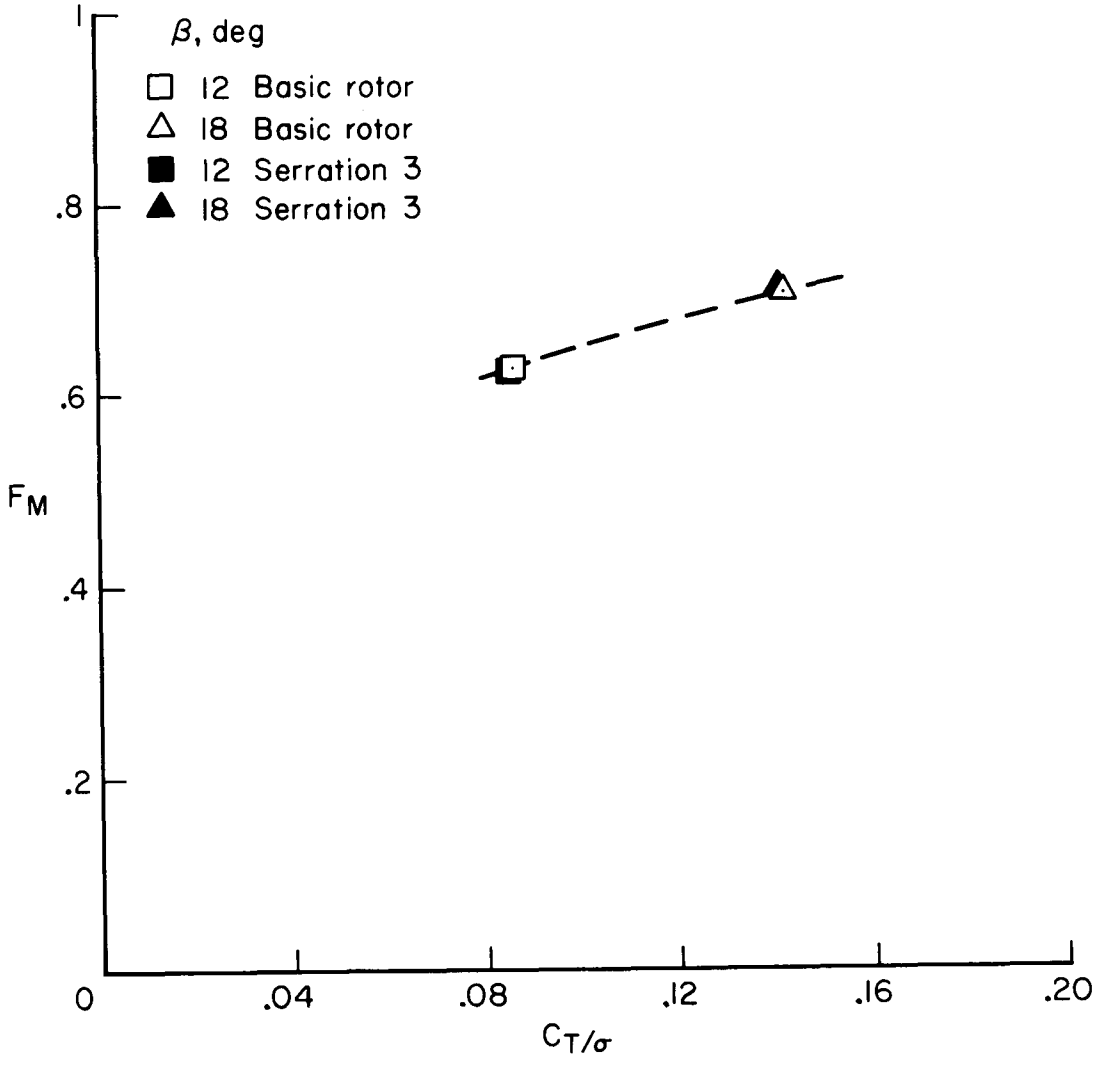

(a) 800 rpm, position 3.

Figure 20.– Figure of merit (F_M) versus C_T/σ for the large-scale rotor, with and without serration 3.

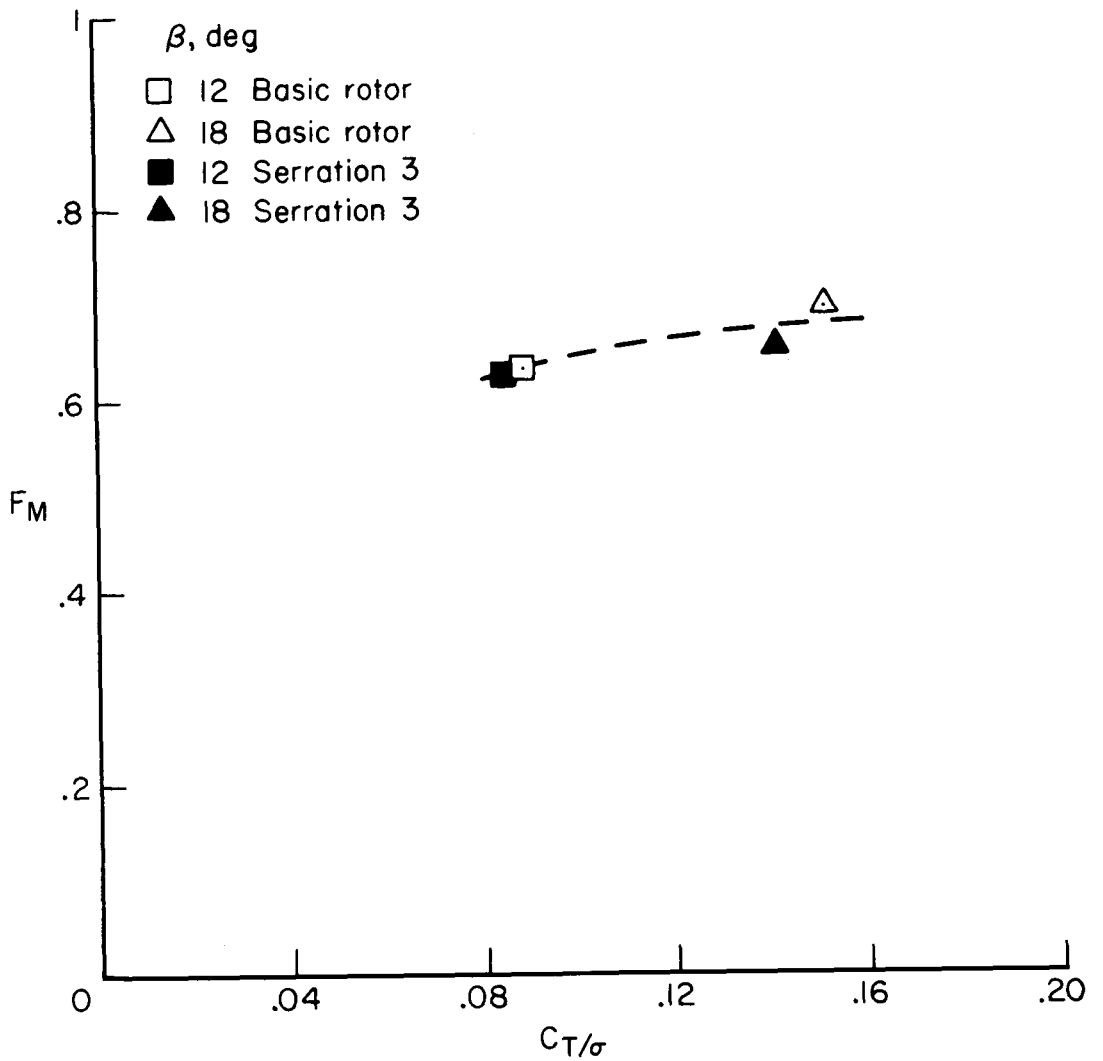

(b) 1000 rpm, position 3.

Figure 20.– Continued.

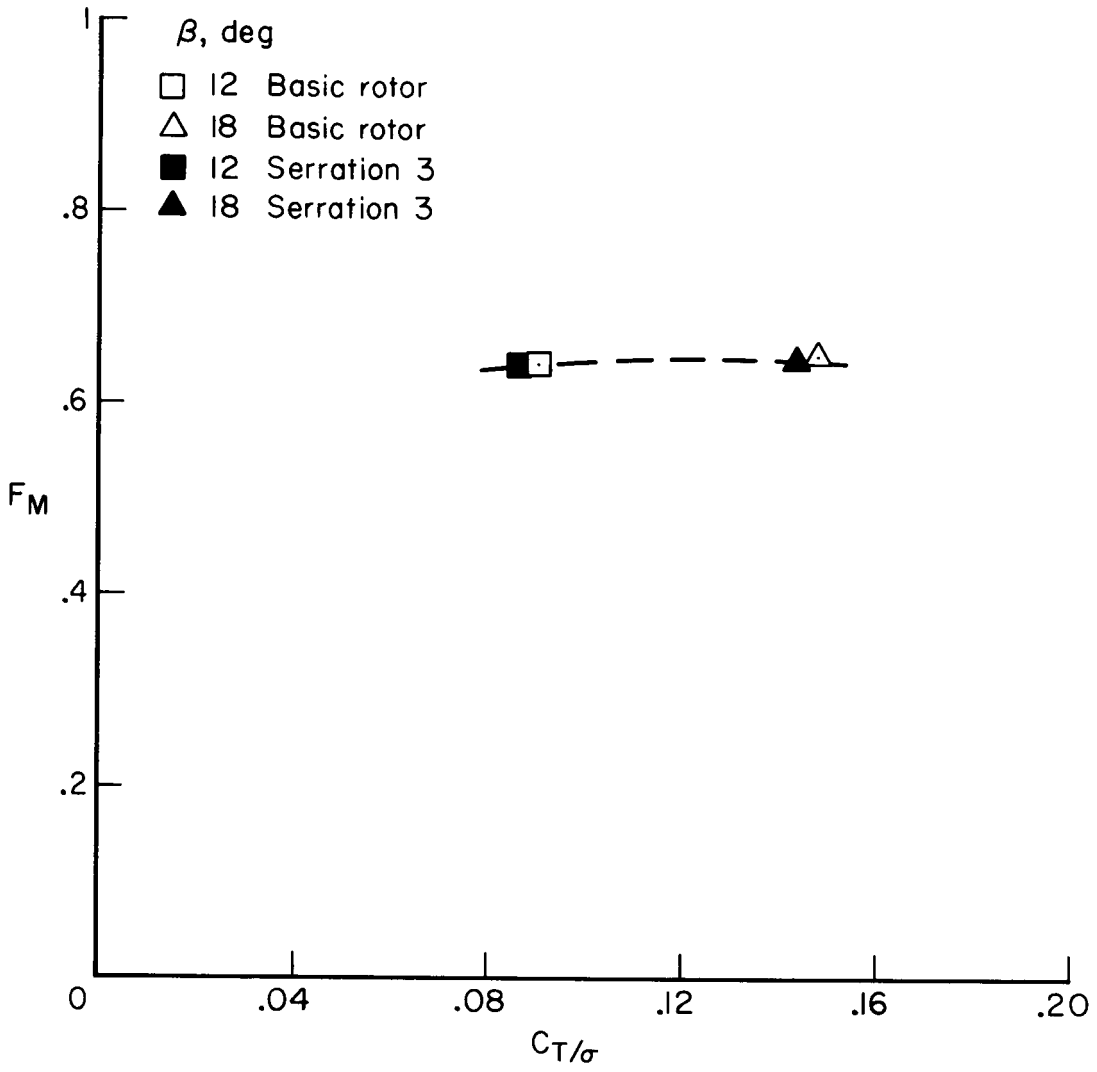

(c) 1400 rpm, position 3.

Figure 20.– Continued.

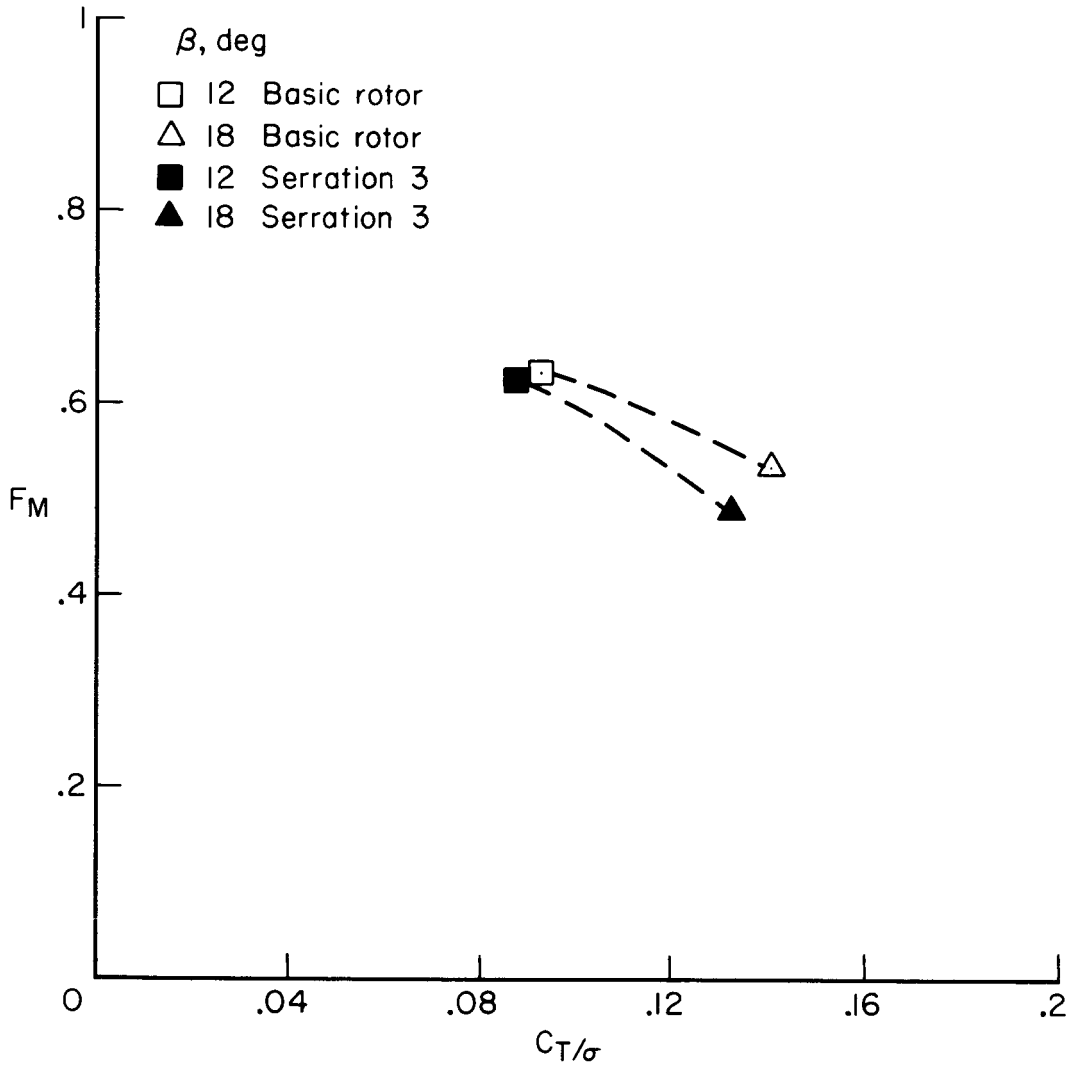

(d) 1600 rpm, position 3.

Figure 20.– Continued.

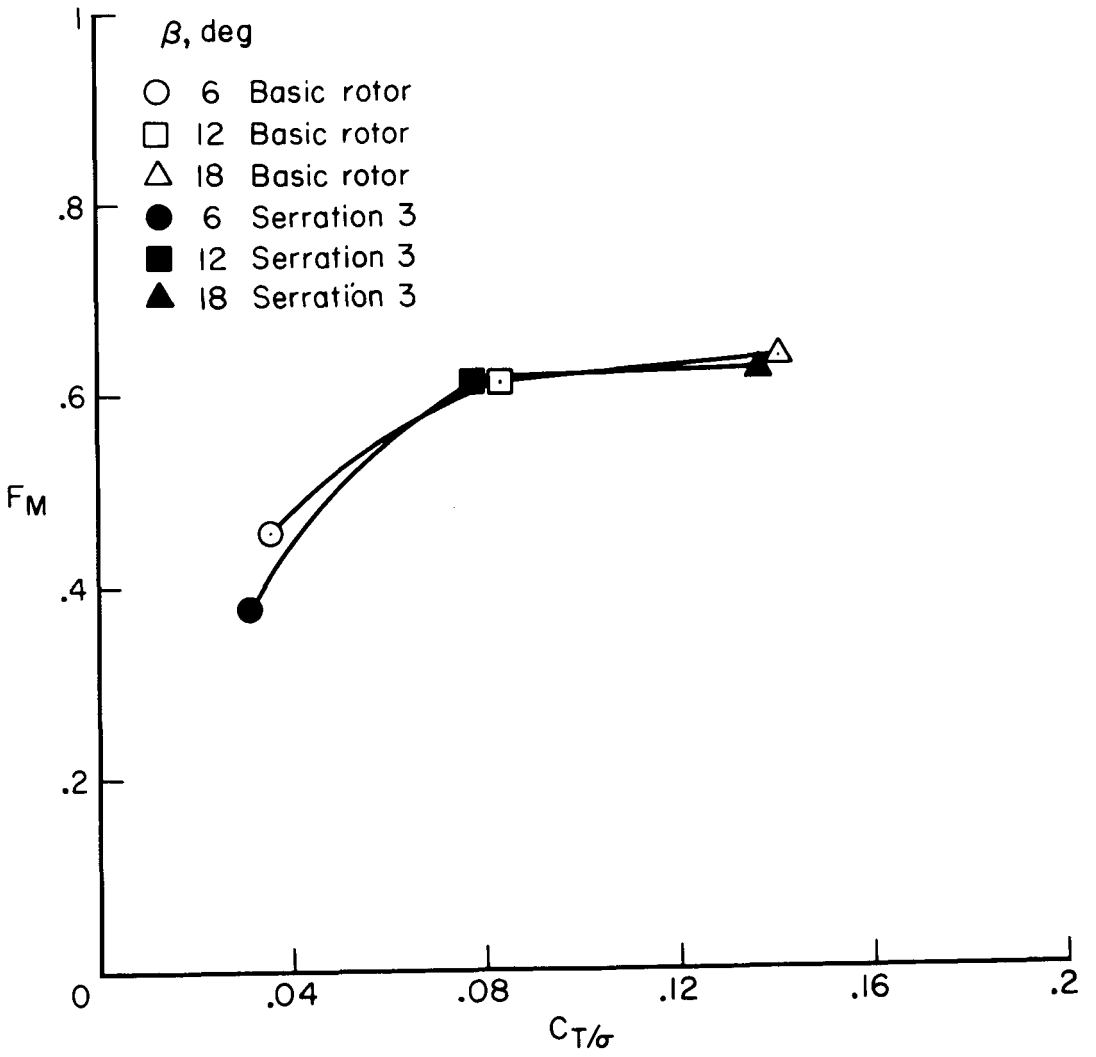

(e) 1400 rpm, position 1.

Figure 20.– Concluded.

NASA-Langley, 1973 —— 2